DEPARTMENT OF DEFENCE
DEFENCE SCIENCE & TECHNOLOGY ORGANISATION
DSTO

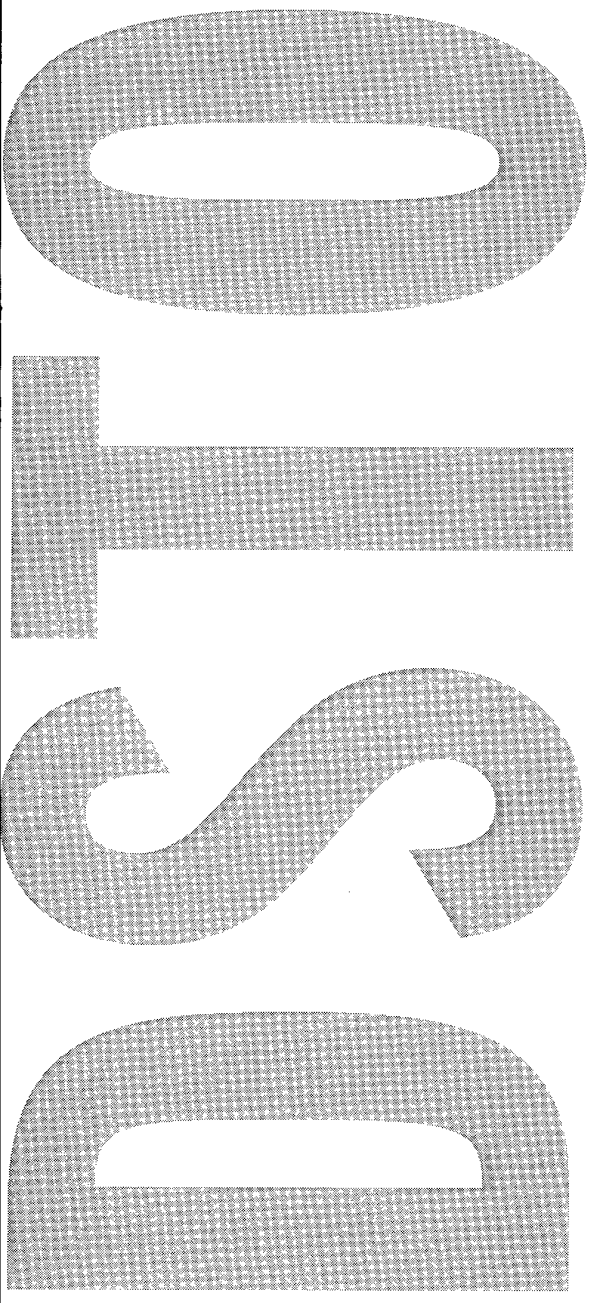

Quantifying Multi-channel Receiver Calibration

G.J. Frazer and Yu.I. Abramovich

DSTO-TR-1152

Quantifying Multi-channel Receiver Calibration

G. J. Frazer and Yu. I. Abramovich

Surveillance Systems Division
Electronics and Surveillance Research Laboratory

DSTO–TR–1152

ABSTRACT

A novel test has been developed for measuring the maximum achievable calibration performance of a multi-channel receiving system. The test may also be used to determine the quality of a particular calibration scheme and to rank the relative performance of several calibration schemes. The test provides a quantitive measure of the dynamic range of the multi-channel receiver. We demonstrate the utility of the test by analysing two different eight channel receiver systems.

Published by

DSTO Electronics and Surveillance Research Laboratory
PO Box 1500
Salisbury, South Australia, Australia 5108

Telephone: *(08) 8259 5555*
Facsimile: *(08) 8259 6567*

AR No. AR 011-867
June, 2001

APPROVED FOR PUBLIC RELEASE

Quantifying Multi-channel Receiver Calibration

EXECUTIVE SUMMARY

Many high frequency radar and communications systems use multi-channel arrays and receivers with digital output for the receiving system. This approach allows multiple simultaneous and adaptive optimal beam coverage implemented using digital beamforming and where each beam is formed by a weighted linear combination of the output of the multi-channel receiver.

Digital beamforming will work correctly provided that a plane wave impinging on the array remains plane following digitisation in the final stage of the receiver. Implementation departures from an ideal design mean that the plane wave requirement will not be achieved exactly and will cause degraded beamformer performance. In most cases the receiver requires explicit calibration to correct this error to reach some desired level of system performance.

An important contributor to calibration error is non-identity between individual channels in the multi-channel receiver. Existing techniques for calibrating multi-channel receivers are based on introducing a training or calibration signal and from measurements of this signal deriving corrective data or calibration tables. These techniques are open loop. There is no explicit assessment of the performance achieved by a given calibration table. At best there is a bad data check. There is also no method for ranking the performance of two candidate calibration tables and no means of determining just how well a particular calibration scheme can improve channel homogeneity given inherent receiver implementation limitations.

A novel test has been developed called the receiver rejection test which uses an injected noise calibration source to give two figures of merit called the *receiver rejection ratio* and the *plane wave rejection ratio*. The test determines the maximum attainable calibration performance of a given multi-channel receiver system and indicates how well a particular calibration scheme performs with respect to this maximum and to other potential calibration schemes. The injected test signal used to conduct the receiver rejection test may be used as a calibration source. The maximum attainable calibration performance can be used as a design specification and equipment acceptance metric for new multi-channel receiver systems. It gives a measure of the attainable dynamic range of the receiver system but does not require that the receiver system be already calibrated in order to make the measurement.

The receiver rejection test has been applied to two eight channel high frequency receivers. The results demonstrate the utility of the test and how it might be applied in actual high frequency radar and communications systems. The technique and a wideband calibration scheme derived from the technique are well suited for incorporation in the next generation of direct digital receiver systems based on analog broadcast band and local station rejection filters, wideband A/D converters and digital down converters. Several areas are identified for further investigation.

Authors

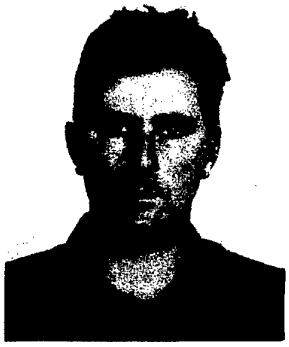

Dr Gordon J. Frazer
Surveillance Systems Division

Dr Frazer received the B.E. (Elect.) (Hons.) degree from the University of Canterbury, New Zealand in 1982, the M.Eng.Sc degree from the University of Queensland, Brisbane in 1990 and the Ph.D degree from Queensland University of Technology, Brisbane in 1996.

From 1982 to 1988 he was a communications engineer with the Queensland Electricity Commission working on communications and control problems in electricity transmission. This included design and implementation of custom modems using digital signal processors. From 1988 until 1990 he developed a variety of custom digital signal processor applications at Mosaic Electronics Pty. Ltd.

Since 1990 he has been with Surveillance Systems Division. He is presently a Senior Research Scientist in Radar Signal Processing Group. His research interests are in array signal processing, signal analysis and radar design.

Professor Yuri I. Abramovich
Surveillance Systems Division

Professor Abramovich received the Dip. Eng. (Hons.) degree in radio electronics in 1967 and the Candidate of Science degree (Ph.D. equivalent) in theoretic radio techniques in 1971, both from the Odessa Polytechnic University, USSR, and in 1981 the D.Sc. degree in radar and navigation from the Leningrad Institute for Avionics.

From 1968 to 1994 he was with the Odessa State Polytechnic University, Ukraine, as a research fellow, professor and finally as Vice-Chancellor of Science and Research. From 1994 to 2000 he was at the Cooperative Research Centre for Sensor Signal and Information Processing (CSSIP) in South Australia as a visiting professor. Since 2000 he has been with Surveillance Systems Division, DSTO, as a Principal Research Scientist and retains his visiting position at CSSIP. His research interests are in the application of signal processing to radar, particularly over-the-horizon radar, electronic warfare and communications, particularly spatio-temporal adaptive processing, beamforming, signal detection and estimation.

Contents

Notation

A/D	analog to digital converter
DDC	digital down converter
DDRX	Direct digital receiver
DSTO	Defence Science and Technology Organisation
FIR	finite impulse response
HF	high frequency (3-30 MHz)
Hz	Hertz
IF	intermediate frequency
KHz	Kilohertz
MVDR	minimum variance distortionless response
MHz	Megahertz
ms	milliseconds
PC	personal computer
RF	radio frequency
Rx	receiver
s	seconds
SSD	Surveillance Systems Division
WJ	Watkins Johnson

1 Introduction

This report considers the problem of quantifying the performance of array calibration schemes in a multi-channel high frequency (HF) radar receiving system. The results reported here are also applicable to HF communications receiving systems although that is not our motivating application.

Array calibration is the compensation of perturbations from ideal and known propagation delays and gains in individual receiver channels in a multi-channel receiving array. These propagation delays and gains are measured from the instant a free space electromagnetic wave impinges on a given array element to the instant the information contained in the electromagnetic wave is digitised in an analog to digital (A/D) converter at the output of the receiver.

Appropriately accurate array calibration (or the synonymic expression array manifold identification) is required for classical beamforming to ensure beam sidelobe levels are tolerably low. It is also required for array systems using adaptive beamforming to ensure errors in knowledge of the preserved "look" direction do not result in desired signal cancellation[1].

In a receiving system comprising more than one element, the following components contribute to finite propagation delay and propagation delay and gain mismatch between channels: antenna element design and positioning, element earthing, pre-amplifier, pre-filter and matching unit design, mutual coupling between elements, mutual coupling with other nearby conductors, feeders, feeder matching, receiver pre-select filters, receiver local oscillator design, receiver intermediate frequency IF design and A/D conversion timing.

We have found it convenient to divide such sources of propagation delay and gain error into two categories. First are those which have approximately constant delay and gain error between channels across the operating bandwidth of the radar. We call this wideband error. Second are those delay and gain errors which vary with frequency across the bandwidth of the radar and which we call narrowband error. Both wideband and narrowband error may vary with radar carrier frequency.

Wideband errors can be minimised by enforcing homogeneity of the antenna and feeder layout. For example, using equal length feeders, rigorous attention to earthing and a linear equi-spaced array including passive elements either within or beyond the array end to minimise the effect of mutual coupling inhomogeneity between elements. Of course some wideband error will remain due to wideband error in components of the multi-channel receiver, for example, differences in pre-select filters between channels.

Subject to these design guidelines, the major source of error is wideband and narrowband error in the receiver, which is generally due to non-identity between the IF and pre-select filters of different channels. Some residual wideband error remains due to the array and feeder system.

In practical HF radar receivers the individual channels are collocated in a central equipment shelter and so the sources of error caused by the receiver are together in one location. This simplifies calibration to remove these errors since it is straightforward to use an injected source in the equipment shelter rather than a radiated calibration source

and attempt to calibrate both the antenna array and the receiver in the presence of sources of external noise and interference.

Existing approaches to calibrating HF radar arrays such as used in the Jindalee skywave radar [2] typically proceed as follows. In the system design phase the wideband errors in the antenna and feeder are minimised by the design and layout techniques listed previously. During operations the radar system generates "calibration tables" using some injected source technique and a specific radar calibration mode to compensate for errors within the receiver. There are checks to overall calibration using radiated sources during installation and major maintenance phases. In these calibration schemes the calibration tables are constructed using an open loop approach. There is no formal check on the "quality" of the generated tables as part of the calibration process except for a rudimentary bad data test.

There are many techniques described in the literature for calibrating arrays for the case of array element position error, for example [3] and the references therein. More appropriate for HF radar is a technique which estimates the directions of arrival of radiated sources in the presence of element position uncertainty, channel gain and phase error and element mutual coupling[4]. This method calibrates the array as part of estimating the directions of arrival.

These techniques are mostly iterative and use externally radiated sources, either co-operatively or otherwise, and are therefore vulnerable to externally radiated interference during calibration. Importantly, none of the methods provide any metric for quantifying the performance of the calibration solution they generate other than apparent convergence of the iterative calibration algorithm.

In this report we address the problem of determining a quality measure to apply when calibrating multi-channel receiver systems. A new technique has been developed which allows one to determine the maximum attainable calibration performance and whether a particular new calibration table is an improvement on a previous calibration table. The technique may also be used as the basis of a scheme to generate new calibration tables although this is not the main purpose. In related work [5] the authors have investigated the achievable performance of a multi-channel receiver equalisation filter which uses circular convolution to implement calibration filters in a computationally efficient manner.

2 Multi-channel receiver specification and calibration

We propose a new test called the receiver rejection test which uses an injected noise calibration source to give two figures of merit. We call these the *receiver rejection ratio* and the *plane wave rejection ratio.* The test determines the maximum attainable calibration performance of a particular multi-channel receiver system and indicates how well a particular calibration scheme performs with respect to this maximum.

The injected test signal used to conduct the receiver rejection test may be used as a calibration source itself, although other sources and techniques are not precluded. For ex-

ample, in an existing radar a calibration scheme may already be in place, the performance of which can be evaluated using the receiver rejection test.

We further propose that the maximum attainable calibration performance can be used as a design specification and equipment acceptance metric for new multi-channel receiver systems. It gives a measure of the attainable dynamic range of the receiver system but does not require that the receiver system be already calibrated in order to make the measurement. This way, specification and testing of new receiver systems can be separated from specification and testing of an array calibration scheme.

2.1 Receiver rejection test

In this section we define our notation and present the receiver rejection test. We then detail how the test is applied in practice and identify important properties of the test, the test equipment configuration and in section 2.1.5 provide interpretation and physical insight. Finally, we provide guidelines for selecting how many array snapshots are required to produce meaningful results.

2.1.1 Definitions

We use the notation that superscript $'$ denotes conjugation, superscript T denotes transpose, superscript H conjugate transpose and $\mathbf{E}$ the expectation operator.

Consider the sampled and digitised output of a one dimensional equi-spaced array of M antenna elements. Let $\mathbf{x}_i = [x_{1,i}, \ldots, x_{M,i}]^T$ be the i^{th} snapshot output from the array, where $i \in [1, \ldots, N]$ for in total N snapshots. Let $X = [\mathbf{x}_1, \ldots, \mathbf{x}_i, \ldots, \mathbf{x}_N]$ be called the data matrix. The covariance matrix is defined as $\mathbf{R} = \mathbf{E}[XX^H]$ while in practice we will use an estimated covariance matrix

$$\hat{\mathbf{R}} = \frac{1}{N} \sum_{i=1}^{N} \mathbf{x}_i \mathbf{x}_i^H \tag{1}$$

Generally, the receiver rejection test evaluates intermediate results, one per receiver channel. We index these by $k \in [1, \ldots, M]$.

Define the *receiver steering vector* for the k^{th} channel $\mathbf{e}_k$ as the $M \times 1$ vector with elements $[e_{1,k}, \ldots, e_{p,k}, \ldots, e_{M,k}]^T$ and where $e_{p,k} = 0$ for $p \neq k$ and $e_{p,k} = 1$ for $p = k$. For example, for the third or $k = 3$ channel in an 8 channel receiver system $\mathbf{e}_3 = [0, 0, 1, 0, 0, 0, 0, 0]^T$.

Similarly define the *plane wave steering vector* for the k^{th} channel $\mathbf{d}_k$ as the $M \times 1$ vector with elements $[d_{1,k}, \ldots, d_{p,k}, \ldots, d_{M,k}]^T$ and where $d_{p,k} = \frac{1}{M-1}$ for $p \neq k$ and $d_{p,k} = -1$ for $p = k$. For example, for the $k = 3$ channel in an 8 channel receiver system $\mathbf{d}_3 = [\frac{1}{7}, \frac{1}{7}, -1, \frac{1}{7}, \frac{1}{7}, \frac{1}{7}, \frac{1}{7}, \frac{1}{7}]^T$

Also define the *calibration weight vector* $\mathbf{c}$ as the $M \times 1$ vector $[c_1, \ldots, c_p, \ldots, c_M]^T$ where for convenience and without loss of generality $c_1 = 1$ and c_p for $p \neq 1$ are determined from some wideband calibration scheme. We note that this a very simple calibration weight model. The *calibration matrix* is defined as $C = \text{diag}(\mathbf{c})$

Let $\mathbf{w}$ be the $M \times 1$ vector with elements $[w_1, \ldots, w_p, \ldots, w_M]^T$ called the *beamformer weight vector* or more concisely the *weight vector*. For a beamformer $y_i = \mathbf{w}^H \mathbf{x}_i$ with output power $\mathbf{E}[|y_i \cdot y_i'|] = \mathbf{w}^H \hat{\mathbf{R}} \mathbf{w}$ the solution to

$$\min_{\mathbf{w}} [\mathbf{w}^H \hat{\mathbf{R}} \mathbf{w}] \tag{2}$$

subject to the unity gain in direction θ constraint

$$\mathbf{t}(\theta)^H \mathbf{w} = 1 \tag{3}$$

for a *steering vector* $\mathbf{t}(\theta)$ is given by the well known minimum variance distortionless response (MVDR) beamformer [6]

$$\mathbf{w}_{\text{opt}} = \frac{\hat{\mathbf{R}}^{-1} \mathbf{t}(\theta)}{\mathbf{t}(\theta)^H \hat{\mathbf{R}}^{-1} \mathbf{t}(\theta)} \tag{4}$$

In this case the steering vector $\mathbf{t}(\theta)$ is of the form $[t(\theta)_1, \ldots, t(\theta)_M]^T$ with the elements determined by the array manifold and the desired steer direction θ. A classical fixed beamformer has a gain of M assuming we ignore loss due to aperture taper. For a MVDR beamformer the gain achieved by the array can not be a useful performance measure since the constraint equation (3) enforces this gain to be unity. Instead, the signal to noise power ratio improvement achieved by the MVDR beamformer is used where this improvement ratio is defined as

$$\hat{G}_{\text{MVDR}} = \frac{\mathbf{e}_1^H \hat{\mathbf{R}} \, \mathbf{e}_1}{\mathbf{w}_{\text{opt}}^H \hat{\mathbf{R}} \, \mathbf{w}_{\text{opt}}} \tag{5}$$

and where the numerator $\mathbf{e}_1^H \hat{\mathbf{R}} \, \mathbf{e}_1$ is the noise output power in the first array channel (i.e. a channel with unity gain) and the denominator $\mathbf{w}_{\text{opt}}^H \hat{\mathbf{R}} \, \mathbf{w}_{\text{opt}}$ is the power which remains following application of the beamformer with weight vector $\mathbf{w}_{\text{opt}}^H$. Actually, this definition applies regardless of the choice of the weight vector. However, if the weight vector is selected using equation (4) and using the true covariance $\mathbf{R}$ and if the signal to noise ratio improvement is calculated using equation (5) and the true covariance then the signal to noise ratio improvement is maximised. We note that $\hat{G}_{\text{MVDR}}$ is a random variable with distribution dependent on the distribution of the estimated covariance $\hat{\mathbf{R}}$. We expand on this in section 2.1.6.

The *receiver rejection test* is defined as the ratio

$$\boxed{r_{\text{rx}} = \frac{1}{M} \sum_{k=0}^{M-1} \frac{\mathbf{e}_k^H \hat{\mathbf{R}} \, \mathbf{e}_k}{\mathbf{w}_{\text{opt},k}^H \hat{\mathbf{R}} \, \mathbf{w}_{\text{opt},k}}} \tag{6}$$

where the k^{th} weight vector $\mathbf{w}_{\text{opt},k}$ is given by the MVDR formula equation (4)

$$\mathbf{w}_{\text{opt},k} = \frac{\hat{\mathbf{R}}^{-1} \mathbf{e}_k}{\mathbf{e}_k^H \hat{\mathbf{R}}^{-1} \mathbf{e}_k} \tag{7}$$

This is the average over all M channels of the ratio of the power in the k^{th} channel $\mathbf{e}_k^H \hat{\mathbf{R}} \, \mathbf{e}_k$ (the numerator in equation (6)) to the power remaining in that channel $\mathbf{w}_{\text{opt},k}^H \hat{\mathbf{R}} \, \mathbf{w}_{\text{opt},k}$ (the denominator in (6)) following application of the optimum beamformer with weight vector

$\mathbf{w}_{\text{opt},k}$. In this case the optimum weight beamformer removes all power which is linearly correlated between receiver channels.

The *plane wave rejection test* is similarly defined as

$$\boxed{r_{\text{pw}} = \frac{1}{M}\sum_{k=0}^{M-1}\frac{\mathbf{e}_k^H\hat{\mathbf{R}}\,\mathbf{e}_k}{\mathbf{d}_k^H\hat{\mathbf{R}}\,\mathbf{d}_k}} \tag{8}$$

This is the average over all M channels of the ratio of the power in the k^{th} channel $\mathbf{e}_k^H\hat{\mathbf{R}}\,\mathbf{e}_k$ to the power remaining in that channel $\mathbf{d}_k^H\hat{\mathbf{R}}\,\mathbf{d}_k$ following application of a beamformer $\mathbf{d}_k$ which only rejects power arriving from boresight.

When calibration weights $\mathbf{c}$ or the calibration matrix C are available, then r_{pw} is given by the modified form

$$r_{\text{pw}} = \frac{1}{M}\sum_{k=0}^{M-1}\frac{\mathbf{e}_k^H C^H\hat{\mathbf{R}}C\,\mathbf{e}_k}{\mathbf{d}_k^H C^H\hat{\mathbf{R}}C\,\mathbf{d}_k} \tag{9}$$

To permit demonstration of the proposed calibration performance metric we have used the following trivial wideband calibration scheme throughout our work

$$c_p = \frac{1}{N}\sum_{i=0}^{N-1}\frac{x_{0,i}}{x_{p,i}} \tag{10}$$

2.1.2 Test procedure

The receiver rejection test proceeds as follows:

1. Inject a broadband (with respect to the Rx passband) noise source through matched amplitude and delay paths into the RF input of each receiver channel and record digitised receiver output data. This is the superposition of a temporally broadband spatially rank one signal and the internal noise of each receiver channel (rank M assuming internal noise contributions from each channel are uncorrelated).
2. Vary the input noise source power level from below the internal noise of the receiver system to a level which is known to generate power in the output caused by non-linearity in the receiver system. This may be caused by compression or saturation or both in the receiver and A/D converter.
3. Record receiver output data (how much data is discussed shortly) for each of a regular set of input noise source power levels. Determine r_{rx} and r_{pw} as a function of the input noise source power level.
4. The maximum r_{rx} indicates the maximum rejectability of the receiver system and is a measure of the dynamic range of the multi-channel receiver.
5. r_{pw} indicates the performance of the current calibration scheme.
6. The noise signal corresponding to the level which achieved maximum r_{rx} is the appropriate signal to use for generating new calibration tables. The external to internal noise power ratio of this noise signal is greatest without being compromised by deleterious effects introduced by non-linearity in the receiver.

2.1.3 Properties

The margin between r_{pw} and r_{rx} gives a measure of the quality of the current calibration scheme. With ideal calibration and using the true covariance $\mathbf{R}$

$$r_{\text{pw}} = r_{\text{rx}} \tag{11}$$

For r_{pw}^{A} and r_{pw}^{B} derived from two different calibration schemes A and B and using the true covariance $\mathbf{R}$, then calibration scheme A is better than scheme B if

$$r_{\text{pw}}^{\text{A}} > r_{\text{pw}}^{\text{B}} \tag{12}$$

and

$$r_{\text{rx}} \geq r_{\text{pw}}^{\text{A}} > r_{\text{pw}}^{\text{B}} \tag{13}$$

In practice we use $\hat{\mathbf{R}}$ in place of $\mathbf{R}$ so r_{rx} and r_{pw} are random variables. The equality and inequalities listed should be considered in relation to the convergence properties of $\hat{\mathbf{R}} \rightarrow \mathbf{R}$.

2.1.4 Test equipment configuration

The receiver rejection test equipment configuration is shown in figure 1. The bandpass filter used in the test had either 25KHz or 200KHz bandwidth at a center frequency of 10.7MHz. Filtering is required because without any band limiting of the noise source it is technically difficult to implement the necessary gain so as to drive the receiver system with enough signal to cause non-linear behaviour. We selected 10.7MHz as the test carrier frequency because of the availability of the two bandpass filters. In general, one or several test carrier frequencies should be examined. The second amplifier was followed by an attenuator with 120dB range in steps of 1dB. Sufficient data snapshots (N) should be collected to ensure that $\hat{\mathbf{R}}$ tolerably approximates $\mathbf{R}$. Guidelines for selecting N are presented in section 2.1.6.

The amplitude gain and delay through the 8 way splitter and the cable paths from the splitter to the receiver under test should be equal. This is required because the definition for the covariance matrix assumes an equally spaced array and the receiver rejection test requires that the noise source is rank one and arriving from boresight.

This is not a significant restriction. Consider a practical calibration system designed to correct calibration errors caused by equipment within the receiver system shelter and which uses our approach as a performance metric. In this case the noise source and splitter equipment will also be collocated with the receiver hardware in the equipment shelter. Irrespective of the actual array geometry it will be possible to treat the calibration measurements as though the array is linear and equi-spaced with arbitrary inter-element spacing. A block diagram of such a system is shown in figure 2.

2.1.5 Interpretation and comments

The ratios r_{rx} and r_{pw} are the average across all channels of the ratio of the power in one receiver channel, the "test" or k^{th} channel, to the power removed from that channel

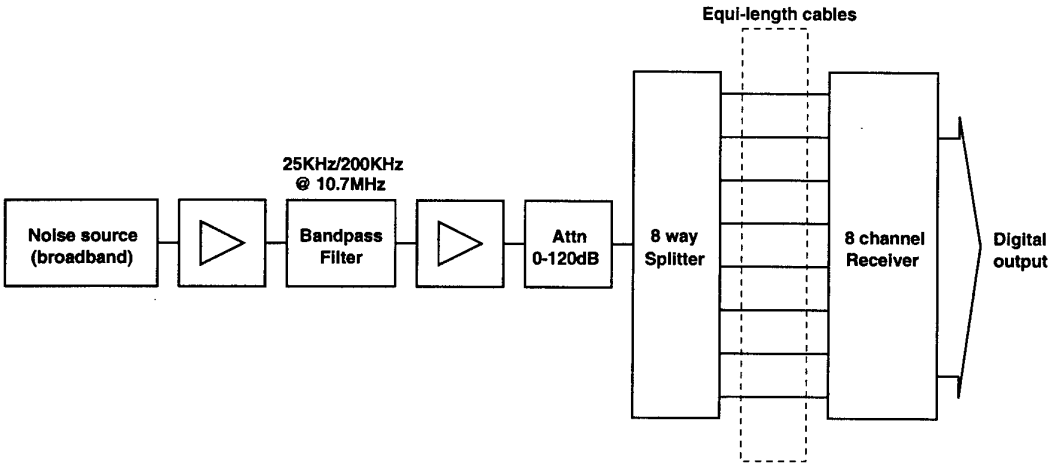

Figure 1: Receiver rejection test laboratory apparatus.

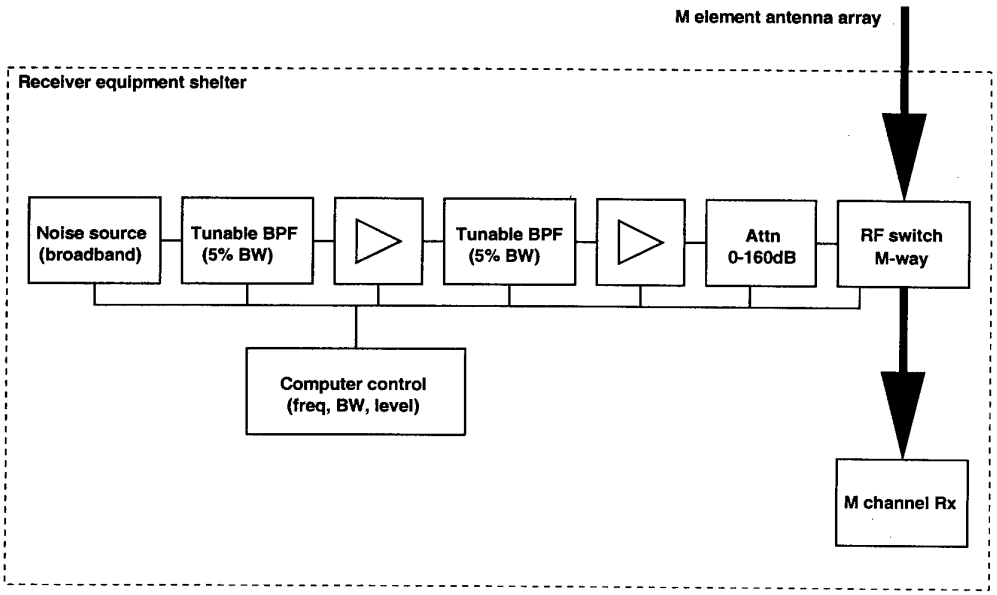

Figure 2: Equipment configuration for a practical calibration scheme.

using a linear combination of the signal measured in the remaining channels. All channels are combined to remove that part of the signal which is coherent across channels, thereby reducing the power in the test channel.

Each channel will contain some noise which is incoherent with respect to other channels. The dominant contribution is from individual receiver channel internal noise. Incoherent noise in the k^{th} channel can not be removed with a linear combination of all M channels. With no external signal (or test noise source) applied, the covariance $\mathbf{R}$ will be full rank and have approximately equal eigenvalues and $r_{\text{rx}} \to 0$ and $r_{\text{pw}} \to 0$.

If the input signal is sufficiently large for any receiver channel to generate output power due to non-linearity effects in the receiver channels then a linear combination of receiver channels will no longer be sufficient to fully reduce the power in the test channel. In this case r_{rx} and r_{pw} will be reduced.

For the *plane wave rejection test* the channel combining weights are prescribed such that the beamformer will only remove maximum power when the coherent signal is arriving directly from boresight. Any channel delay deviations, such as poor calibration, will reduce the rejection ratio.

For the *receiver rejection test* the beamformer weight vector $\mathbf{w}_{\text{opt},k}$ is optimally chosen to minimise the total output power. This will be achieved regardless of any calibration error given the choice of $\mathbf{e}_k$ as the steering vector. *Selection of* $\mathbf{e}_k$ *as the steering vector is the key to our approach.* Minimum total output power can be achieved with zero desired signal cancellation, *without* requiring that the array be already calibrated.

A narrowband receiver rejection test $r(f)_{\text{rx}}$ can be defined by constructing $\hat{\mathbf{R}}(f)$ from channelised snapshots in the obvious manner. In the two receivers tested so far we have found that while this narrowband extension provides insight into aspects of the operation of the receivers the standard and less complex receiver rejection test has proven sufficient as a performance metric.

2.1.6 Guidelines for selecting the number of snapshots N

In section 2.1.1 it was explained that since the gain of a MVDR beamformer is constrained to be unity the array gain can not be a useful performance measure. An appropriate measure is in fact the signal to noise ratio improvement achieved by the application of a particular weight vector. Maximum signal to noise ratio improvement is achieved when the weight vector is chosen according to the MVDR design formula equation (4).

The MVDR signal to noise ratio improvement measure for the case of a known covariance $\mathbf{R}$ is the deterministic quantity G_{MVDR}

$$G_{\text{MVDR}} = \frac{\mathbf{e}_1^H \mathbf{R}\, \mathbf{e}_1}{\mathbf{w}_{\text{opt}}^H \mathbf{R}\, \mathbf{w}_{\text{opt}}} \tag{14}$$

which is the ratio of the power in one channel $\mathbf{e}_1^H \mathbf{R}\, \mathbf{e}_1$ to the power $\mathbf{w}_{\text{opt}}^H \mathbf{R}\, \mathbf{w}_{\text{opt}}$ remaining following application of the beamformer. In practical applications $\mathbf{R}$ is unknown and one uses the estimated covariance $\hat{\mathbf{R}}$, equation (1) and repeated here

$$\hat{\mathbf{R}} = \frac{1}{N} \sum_{i=1}^{N} \mathbf{x}_i \mathbf{x}_i^H \tag{15}$$

which is formed from N independent snapshots of the data. In this case $\hat{G}_{\text{MVDR}}$ is now a random variable given by (repeated from equation (5))

$$\hat{G}_{\text{MVDR}} = \frac{\mathbf{e}_1^H \hat{\mathbf{R}}\, \mathbf{e}_1}{\mathbf{w}_{\text{opt}}^H \hat{\mathbf{R}}\, \mathbf{w}_{\text{opt}}} \tag{16}$$

In a significant contribution Reed et. al. [7] showed that

$$\hat{G}_{\text{MVDR}} = G_{\text{MVDR}} \cdot \rho(\hat{\mathbf{R}}) \tag{17}$$

where $\rho(\hat{\mathbf{R}})$ is a beta function distributed random variable which takes on values between 0 and 1 under the assumption that the data snapshots used to construct $\hat{\mathbf{R}}$ and hence $\mathbf{w}_{\text{opt}}$ in equation (4) which is used in equation (16) are independent (i.e. different) of the data snapshots used to construct $\hat{\mathbf{R}}$ in equation (16).

$\rho(\hat{\mathbf{R}})$ has mean and variance [8] given by

$$\mathbf{E}[\rho(\hat{\mathbf{R}})] = \frac{N+2-M}{N+1} \tag{18}$$

and

$$\mathbf{E}[\rho^2(\hat{\mathbf{R}})] = \frac{(N+2-M)(M-1)}{(N+1)^2(N+2)} \tag{19}$$

respectively. Note that the expression for $\mathbf{E}[\rho^2(\hat{\mathbf{R}})]$ given in [7] is incorrect. Clearly both $\mathbf{E}[\rho] \to 1$ and $\mathbf{E}[\rho^2] \to 0$ as the number of snapshots N significantly exceeds M in which case $\hat{G}_{\text{MVDR}}$ well approximates G_{MVDR}.

Both the receiver rejection ratio, equation (6), and the plane wave rejection ratio, equation (8), are averages formed from power ratios such as equation (16) and so we can use the advice contained in equation (18) and equation (19) to assist our selection of the required number of snapshots N for a given application. Since we have investigated two eight channel ($M = 8$) receiver systems we have tabulated values of $\mathbf{E}[\rho]$ and $\mathbf{E}[\rho^2]$ for various N in table 1. For $N = 160 = 20 \cdot M$ and larger the expected signal to noise ratio loss and the variance of this loss is very small indeed.

In table 2 we summarise our recommendations for choice of N for three candidate applications relevant to HF radar and communications. We stress that the rate at which independent snapshots may be collected is determined by the post receiver bandwidth of the test noise source and not the sampling rate of the acquisition system. For the system bandwidths typically used in HF radar and communications systems table 2 shows that the selection of the number of snapshots according to the comparatively conservative criteria $\frac{N}{M} \geq 100$ produces snapshot integration intervals which are appropriate for these applications. From table 1 we see that for our recommended selection the expected value of the signal to noise ratio loss with respect to the true value of the signal to noise ratio is 0.04dB and that the variance of this loss is approximately 10^{-5} times the true value of the signal to noise ratio.

In the narrowband receiver rejection test $r(f)_{\text{rx}}$ the estimated covariance $\hat{\mathbf{R}}(f)$ is generated from channelised snapshots output from some digital filter bank. If the bandwidth of each filter in the filter bank is B_{fb} then the rate at which independent snapshots are generated is determined by this bandwidth and not the original noise source bandwidth B_{NS}.

N	$\mathbf{E}[\rho]$	$\mathbf{E}[\rho^2]$ $(\cdot 10^{-3})$	-10 · log $[\mathbf{E}[\rho]]$ (dB)
9	0.3000	19.0909	5.2288
16	0.5882	13.4564	2.3045
40	0.8293	3.3710	0.8130
80	0.9136	0.9628	0.3925
160	0.9565	0.2567	0.1931
320	0.9782	0.0662	0.0958
800	0.9913	0.0108	0.0381
1600	0.9956	0.0027	0.0190
4000	0.9983	0.0004	0.0076
8000	0.9991	0.0001	0.0038
40000	0.9998	0.0000	0.0008
102400	0.9999	0.0000	0.0003

Table 1: Mean and variance of ρ and expected signal to noise ratio loss in dB for various values of N for the case of $M = 8$.

B_{NS} (KHz)	f_s (KHz)	$\frac{N}{M}$	N for $M = 8$	T_{I} (ms)
3.4	>3.4	100	800	235
10	>10	100	800	80
100	>100	100	800	8

Table 2: Recommended selections for N for three typical HF radar and communications scenarios. B_{NS} is the bandwidth of the test noise source. f_s is the complex sampling frequency. T_I is the recommended integration interval for the eight channel case (where $M = 8$).

In general $B_{\mathrm{NS}} > B_{\mathrm{fb}}$ and consequently the narrowband receiver rejection test requires significantly more $(\times \frac{B_{\mathrm{NS}}}{B_{\mathrm{fb}}})$ snapshots than the receiver rejection test. This may mean that our guideline of $\frac{N}{M} \geq 100$ may need to be relaxed and specific values for N investigated for expected value of loss and variance of loss.

3 Results

We have applied the receiver rejection test to two 8 channel HF receiver systems. In this section we provide details of the two receivers tested, present the results obtained, provide an interpretation of these results and demonstrate the influence of varying the number of snapshots N used to form the estimated covariance matrix.

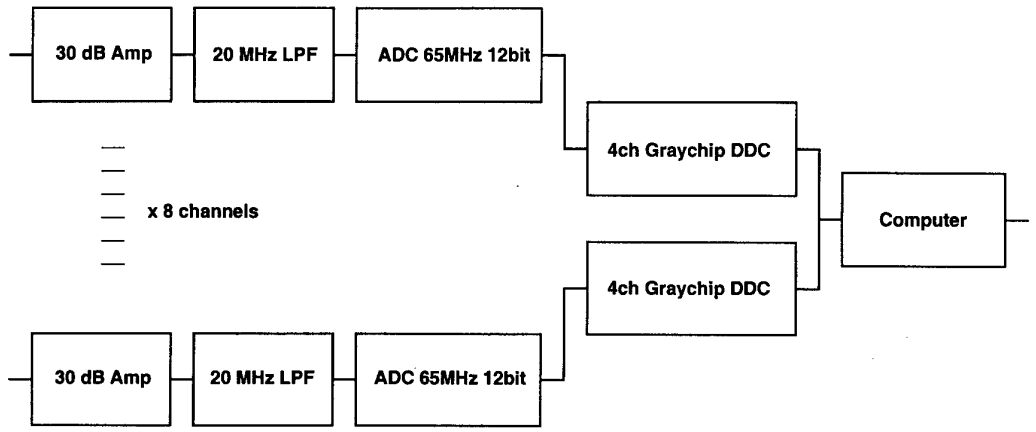

Figure 3: DDRX block diagram.

3.1 Receiver details

3.1.1 DDRX

DDRX is an 8 channel direct digital receiver developed by Communications Division DSTO using Analog Devices and Graychip evaluation modules. It uses 8 x 65MHz 12bit A/D + 2 x 4 ch. Graychip digital down converters. There are lowpass filters with cut-off at 20MHz and 30dB gain amplifiers on the input of each channel. Output data is recorded and the receiver controlled using a PC. A block diagram is shown in figure 3. The DDRX output bandwidth was selected to be 10KHz at a sampling rate (complex) of 10KHz. The coherent measurement interval was 5s. Calibration involved determining one complex weight per channel. Calibration weights were determined from the data set which indicated the highest receiver rejection ratio.

3.1.2 WJ9010

The WJ9010 is an 8 channel HF direction-finding system manufactured by Watkins-Johnson. Each receiver channel uses an analog IF strip, with bandwidth 16KHz. Baseband conversion and filtering and conversion to digital samples is implemented using a built-in 16 bit A/D and digital signal processor chip. The WJ9010 output bandwidth was selected to be 10.4KHz at a sampling rate of 25KHz (complex). The coherent measurement interval was 5s. The WJ9010 has an internal self calibration scheme. Immediately prior to and then immediately following a coherent measurement the WJ9010 internally determines pre and post calibration weights which may be applied to the measured data, or not, at the operators discretion.

3.2 Experimental results

3.2.1 DDRX

The rejection ratios versus noise input power level for the DDRX are shown in figures 5 and 6 for noise source bandwidths of 25KHz and 200KHz respectively. Each figure shows r_{rx} and then r_{pw} for the case of no calibration and following calibration.

Figures 7 through 14 show beampatterns for varying input noise power levels computed for both the calibrated and uncalibrated data sets. The beam patterns show beamformed power versus angle of arrival and have been evaluated on an angle interval of $[-90, 90]$ degrees in 0.1 degree increments. The beampatterns have all been formed using a 50dB Taylor window.

We repeated the beampattern calculations with an 80dB Taylor window. This allowed extraction of the beam peak to maximum sidelobe level ratio without the result saturating at the equi-ripple sidelobe level of the 50dB Taylor window. Figure 15 shows the beam peak to maximum sidelobe level ratio for the calibrated and uncalibrated cases. This data was collected using the 25KHz filter.

Figures 16 and 17 show the uncalibrated and calibrated receiver channel gain transfer function for the DDRX computed with respect to channel 1. Gain difference between channels have reduced to below 0.1dB. Similarly figures 18 and 19 show the uncalibrated and calibrated receiver channel phase transfer function and in this case the inter-channel phase differences are less than 0.2 degrees. Following calibration the receiver channels are close to identical.

3.2.2 WJ9010

The rejection ratios versus noise input power level for the WJ9010 is shown in figures 20 and 21 for noise source bandwidths of 25KHz and 200KHz respectively. Each figure shows r_{rx} and then r_{pw} for the case of no calibration (or uncalibrated), the WJ pre and post calibration (in subsequent investigations we used pre-calibrated only) and finally re-calibration where the simple wideband calibration scheme is applied.

Figures 22 through 30 show beampatterns for varying input noise power levels computed for the uncalibrated, the pre-calibrated and the re-calibrated data sets. The beam patterns show beamformed power versus angle of arrival and have been evaluated on an angle interval of $[-90, 90]$ degrees in 0.1 degree increments. The beampatterns have all been formed using a 50dB Taylor window.

Again we repeated the beampattern calculations with an 80dB Taylor window to give the beam peak to maximum sidelobe level ratio. Figure 31 shows this ratio for the uncalibrated, the pre-calibrated and the re-calibrated cases collected using the 25KHz filter.

Figures 32 and 33 show the pre-calibrated and re-calibrated receiver channel gain transfer function for the WJ9010 computed with respect to channel 1. Average gain difference between channels has reduced. Similarly figures 34 and 35 show the pre-calibrated and re-calibrated receiver channel phase transfer function and in this case the average inter-channel phase differences are also reduced. Significant narrowband gain and phase

non-identity between channels remains and this causes the significant margin between the re-calibrated plane wave rejection ratio and the receiver rejection ratio shown in figure 20.

3.3 Interpretation

The DDRX performs poorly without calibration. It contains a wideband error due to delay and amplitude mismatch in the individual channel amplifier and lowpass filter sets, and possibly errors in the 8-way splitter.

If the latter is the case then this is a test measurement instrument error. We recommend that resistive power splitters should be used in the test equipment instead of transformer based devices. While having greater attenuation resistive power splitters can be constructed with very accurate gain and delay matching between channels compared with transformer based units.

The DDRX beam sidelobe levels decreased following calibration by up to 40dB (see figure 15). This is a substantial improvement which diminishes once the receiver is overdriven into its non-linear operating region.

The calibration error is a broadband effect, since simple 8 complex number calibration has improved calibration such that r_{pw} is close to r_{rx}. This is because the frequency selective filters in the DDRX are well matched digital linear phase FIR filters in the DDC.

The bandwidth of the noise source was selected to be either 200KHz or 25KHz by selecting an appropriate filter at a center frequency of 10.7MHz. Both are greater than the WJ9010 IF bandwidth and so made little difference to the measurements with this receiver. The DDRX has no narrowband analog selectivity in front of the A/D converters and the 200KHz bandwidth noise source reduced the effective dynamic range of the receiver by approximately 10dB compared to the 25KHz bandwidth case. The dominant non-linearity in the DDRX is amplitude clipping in the A/D converters. The 200KHz noise source will produce a peak amplitude approximately 10dB [1] larger than the peak amplitude of the 25KHz noise source when each is observed for the same measurement interval.

The dynamic range of the DDRX is significantly effected by the large signal out-of-band HF environment. A practically useful direct digital receiver system will require analog front end filters for broadcast and local station rejection. Non-identity between the filters of different receiver channels will be a source of wideband calibration error. Since the receiver and the analog front end filters can be expected to be collocated in an equipment shelter the technique based on using an injected calibration source developed here will be able to fully calibrate the receiver system.

The dynamic range limiting mechanisms of the DDRX and the WJ9010 are different and the WJ9010 is less sensitive to the external large signal environment.

The WJ9010 is effectively useless without at least applying either the in-built pre or post measurement calibration weights. There is little difference between the performance of the pre or the post measurement weights. However, both can be improved by further simple 8 complex number calibration, which gives an approximately 5dB reduction in beam sidelobes (see figure 31).

[1] $10\log \frac{200}{25}$

Further improvement again is possible since $\frac{r_{rx}}{r_{pw}}$ is often greater than 10dB. The individual receiver channel transfer functions (measured with respect to channel 1) show that the remaining calibration error is a function of passband frequency. Further calibration improvement will require frequency (within the passband) selective calibration. More sophisticated calibration schemes using a finite impulse response (FIR) filter structure are possible. Determination of FIR equaliser weights is non-trivial. Simple frequency domain (receiver passband) point constraints, say on a regular discrete grid of frequencies, produce poor results due to unconstrained behaviour of the equaliser between the points in the discrete frequency grid. See [5] for consideration of this problem assuming calibration filters implemented using circular convolution.

3.4 Effect of number of snapshots N

The influence of the number of snapshots used to form the estimated covariance $\hat{\mathbf{R}}$ is shown in figures 36 through 41. The receiver rejection test was repeated using the DDRX data for the case of the following set of numbers of snapshots

$$N \in \{9, 16, 40, 80, 160, 320, 800, 1600, 4000, 8000, 40000, 102400\} \tag{20}$$

which, for $M = 8$ receiver channels, correspond to the following multiples of M

$$\frac{N}{M} \in \{1 + 1, 2, 5, 10, 20, 40, 100, 200, 500, 1000, 5000, 12800\} \tag{21}$$

The expected penalty associated with these choices for N is shown in table 1. By $N = 800$ the results are indistinguishable from the $N = 102400$ case. In our experiment we have violated the assumption that the data snapshots used to determine the optimum weight vector are independent from the data snapshots used to construct the estimated covariance matrix which is in turn used to determine the signal to noise power ratio. This certainly effects the small N cases but does not invalidate the number of snapshot selection guidelines proposed earlier. Clearly convergence has been achieved according to our guidelines.

4 Future work

The results of our experiments demonstrate that the receiver rejection test is useful for specifying and calibrating multi-channel receivers. Areas identified for future work include:

1. Develop a narrowband calibration scheme for the WJ9010. The goal is to achieve r_{pw} close to r_{rx} for the WJ9010 and so reduce narrowband (passband) errors.
2. Investigate the influence of M on r_{rx} and r_{pw}. It is expected that both will decrease as $M \to 2$ and the MVDR beamformer "uses up" the M available degrees of freedom rejecting the uncalibrated and hence non-rank one test source.

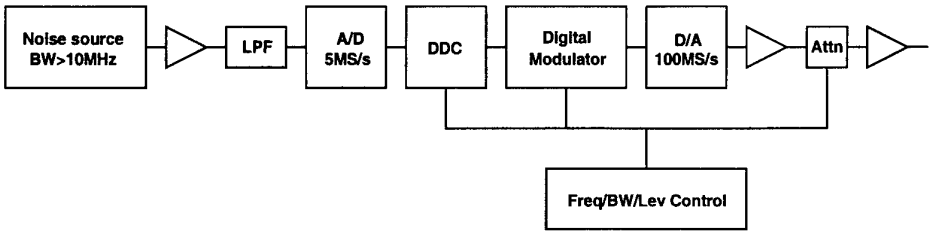

Figure 4: Block diagram of a narrowband direct RF noise source suitable for a radiated receiver rejection test.

3. Investigate the related performance dependence of r_{rx} for the case of $P > 1$ uncorrelated test sources arriving from different angles as $P \to M$. It is expected that this will show the receiver rejection test should be extended to indicate reduced receiver performance for systems designed to operate in the presence of multiple interference sources where the number of sources $P \to M$.

4. Develop a noise source generator suitable for external radiation tests. This requires sufficient output power and accurate bandwidth control. One possible design is outlined in figure 4.

5 Conclusions

We have developed a test for measuring both the maximum achievable calibration performance and the dynamic range of a multi-channel receiving system. The test can also be used to determine the quality of a particular calibration scheme. The technique has been successfully applied to two 8 channel receiving systems.

The technique and a simple wideband error calibration scheme derived from the technique are well suited for incorporation in the next generation of direct digital receiver systems based on analog broadcast band and local station rejection filters, wideband A/D converters and digital down converters.

6 Acknowledgements

Thank you particularly to Mr Geoff Warne for hardware and experimental support, and for a great deal of patience. Thank you also to Mr Dallas Taylor and Mr Ian Zahorvjko for access to the DDRX and the WJ9010 and assistance conducting the experiments. Dallas and Ian's involvement has been made possible under the auspices of the DSTO RF Hub. Thank you to the staff of the Radar Frequency Projects (RFP) Group in SSD for a variety of impositions. Finally thanks to the reviewer Dr Mike Turley for comments which significantly improved the quality of this report.

References

1. A. M. Vural, "Effects of perturbations on the performance of optimum/adaptive arrays," *IEEE Transactions on Aerospace and Electronic Systems*, vol. AES-15, pp. 76–87, January 1979.

2. M. L. Lees, "Digital beamforming calibration for FMCW radar," *IEEE Transactions on Aerospace and Electronic Systems*, vol. 25, pp. 281–284, March 1989.

3. B. P. Ng, M. H. Er, and C. Kot, "Array gain/phase calibration techniques for adaptive beamforming and direction finding," *IEE Proceedings – Radar, Sonar and Navigation*, vol. 141, pp. 25–29, February 1994.

4. B. Friedlander and A. J. Weiss, "Direction finding in the presence of mutual coupling," *IEEE Transactions on Antennas and Propagation*, vol. 39, pp. 273–284, March 1991.

5. Y. I. Abramovich, V. G. Kachur, and V. F. Struchev, "Methods of digital channel correction in multi-channel radar receivers," *Radiotekhnika i electronika*, no. 8, pp. 1544–1550, 1984.

6. J. Capon, "High resolution frequency-wavenumber spectral analysis," *Proceedings of the IEEE*, vol. 57, pp. 1408–1418, August 1969.

7. I. S. Reed, J. D. Mallett, and L. E. Brennan, "Rapid convergence rate in adaptive arrays," *IEEE Transactions on Aerospace and Electronic Systems*, vol. AES-10, pp. 853–863, November 1974.

8. M. Evans, N. Hastings, and B. Peacock, *Statistical Distributions*. John Wiley and Sons, Inc, 2nd ed., 1993.

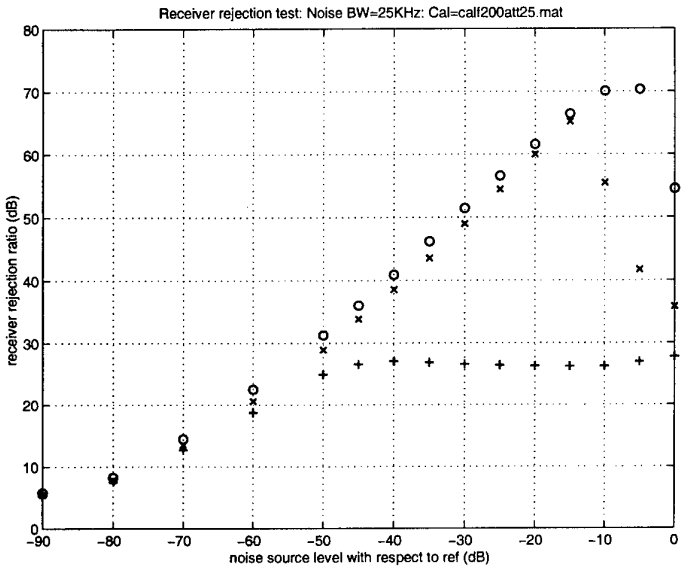

Figure 5: DDRX. (O) receiver rejection ratio. (+) uncalibrated plane wave rejection ratio. (X) calibrated plane wave rejection ratio. Noise source bandwidth 25KHz.

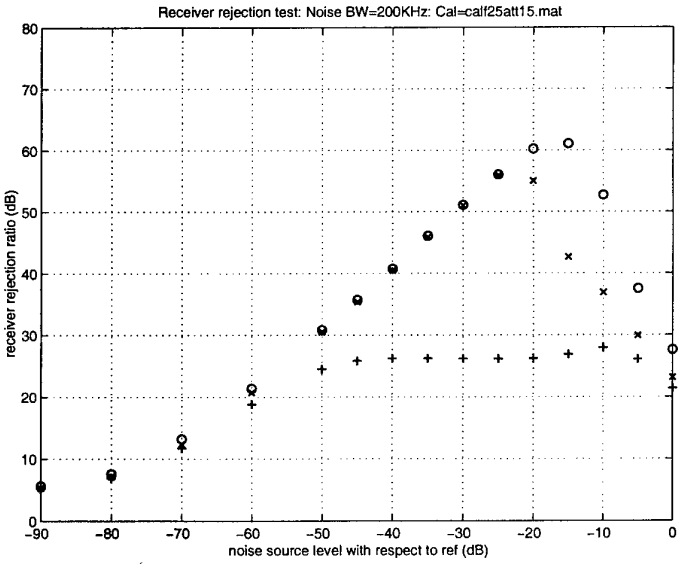

Figure 6: DDRX. (O) receiver rejection ratio. (+) uncalibrated plane wave rejection ratio. (X) calibrated plane wave rejection ratio. Noise source bandwidth 200KHz.

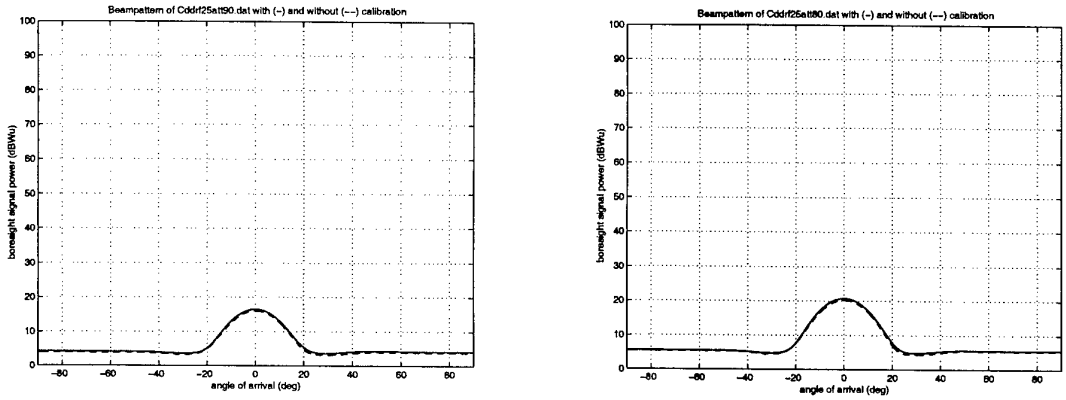

Figure 7: DDRX beampattern. Noise source input level (left) ref-90dB (right) ref-80dB. Noise source bandwidth 25KHz. (-) calibrated. (--) uncalibrated.

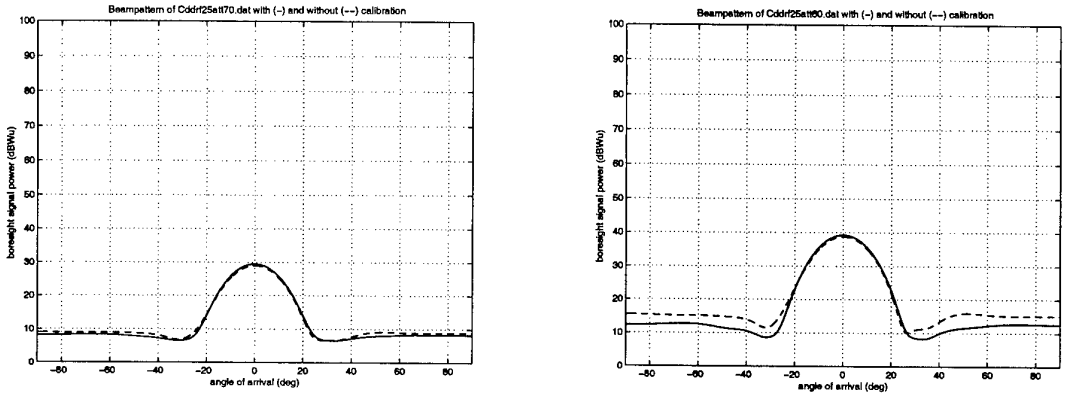

Figure 8: DDRX beampattern. Noise source input level (left) ref-70dB (right) ref-60dB. Noise source bandwidth 25KHz. (-) calibrated. (--) uncalibrated.

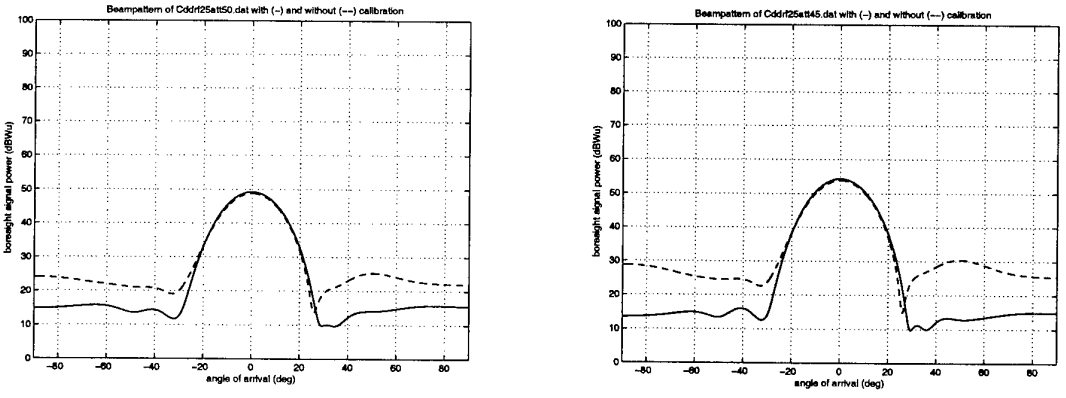

Figure 9: DDRX beampattern. Noise source input level (left) ref-50dB (right) ref-45dB. Noise source bandwidth 25KHz. (-) calibrated. (--) uncalibrated.

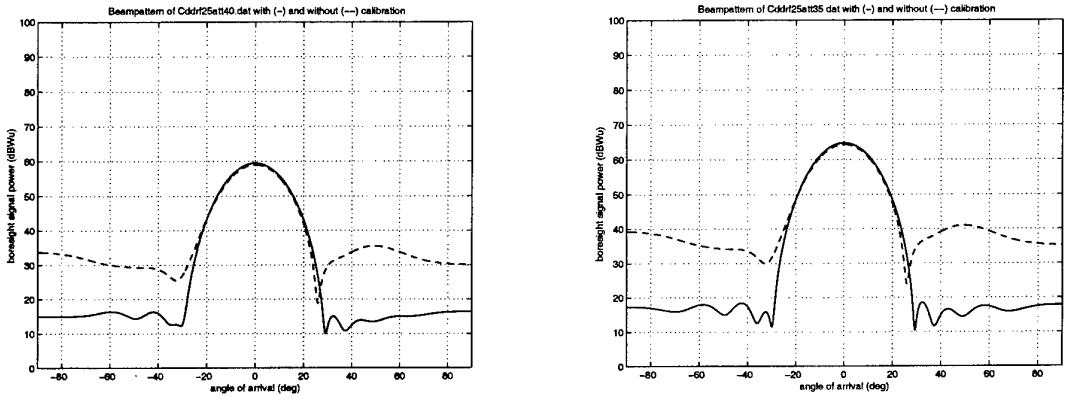

Figure 10: DDRX beampattern. Noise source input level (left) ref-40dB (right) ref-35dB. Noise source bandwidth 25KHz. (-) calibrated. (--) uncalibrated.

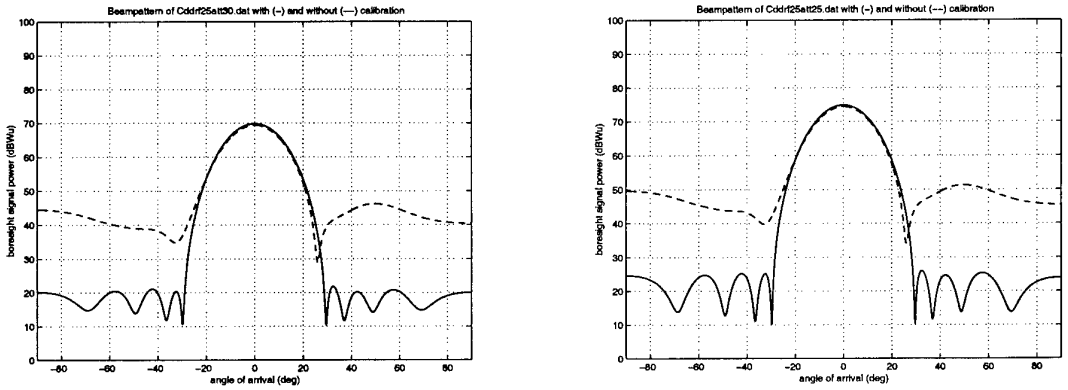

Figure 11: DDRX beampattern. Noise source input level (left) ref-30dB (right) ref-25dB. Noise source bandwidth 25KHz. (-) calibrated. (--) uncalibrated.

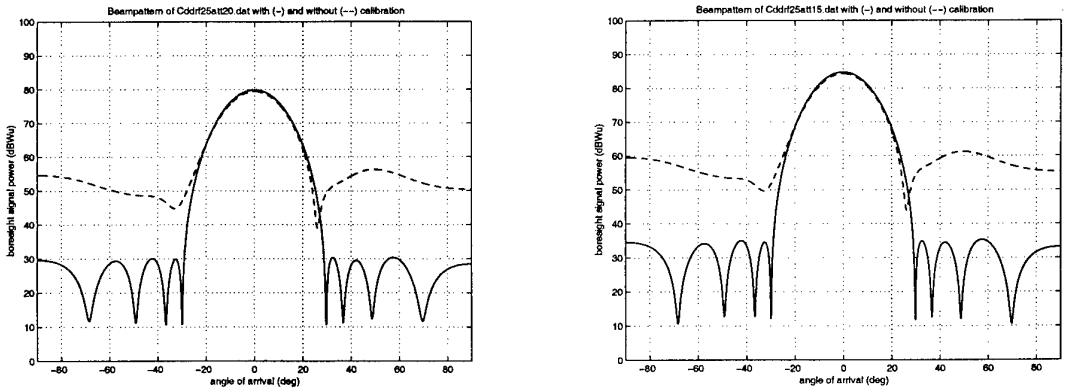

Figure 12: DDRX beampattern. Noise source input level (left) ref-20dB (right) ref-15dB. Noise source bandwidth 25KHz. (-) calibrated. (--) uncalibrated.

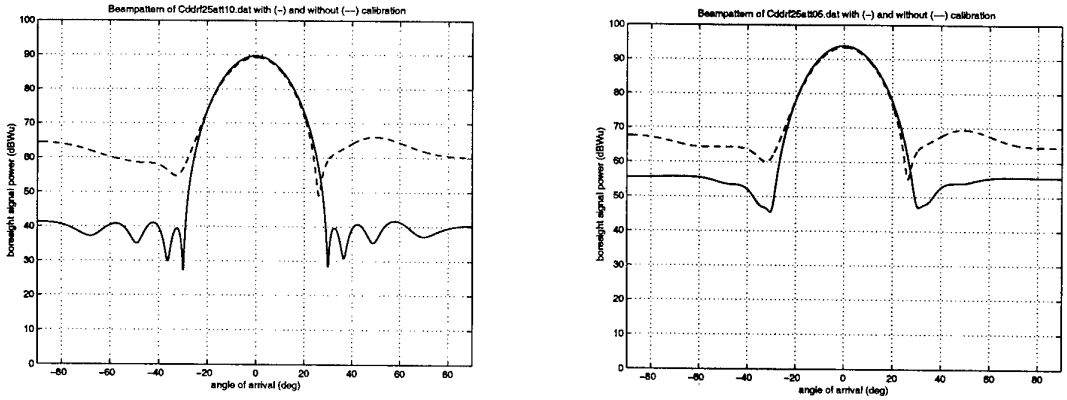

Figure 13: DDRX beampattern. Noise source input level (left) ref-10dB (right) ref-05dB. Noise source bandwidth 25KHz. (-) calibrated. (--) uncalibrated.

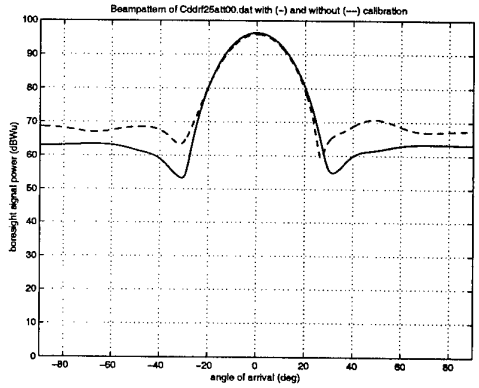

Figure 14: DDRX beampattern. Noise source input level ref-0dB. Noise source bandwidth 25KHz. (-) calibrated. (--) uncalibrated.

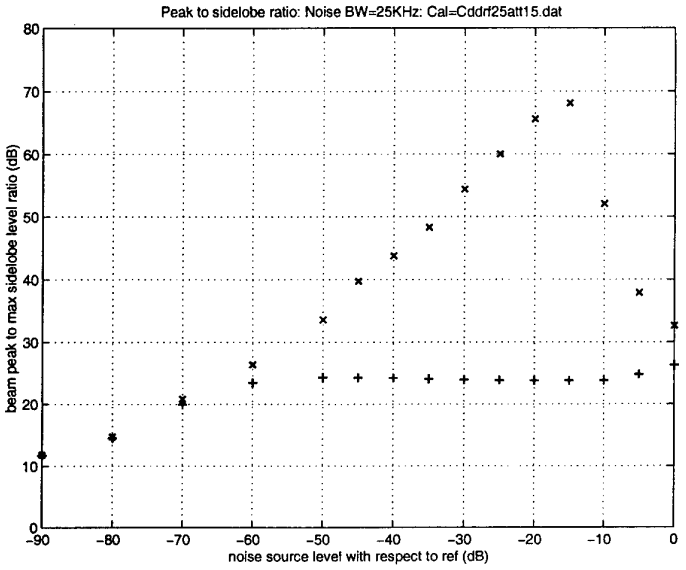

Figure 15: DDRX beam peak to maximum sidelobe level ratio for the (x) calibrated and (+) uncalibrated cases.

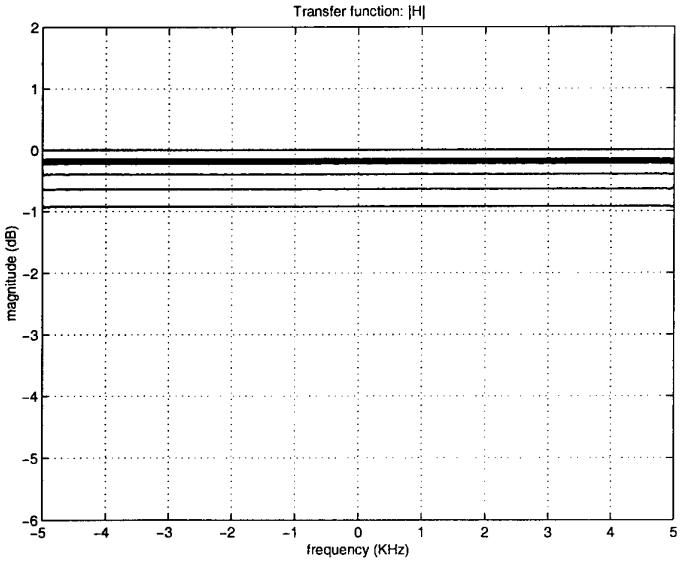

Figure 16: DDRX channel transfer functions (gain) (baseband freq. v. dB) for the uncalibrated case. Multiple lines are individual channels.

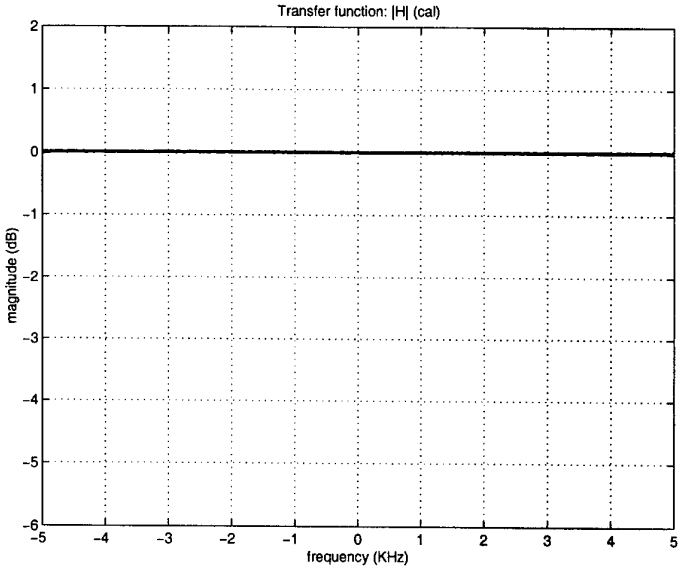

Figure 17: DDRX channel transfer functions (gain) (baseband freq. v. dB) for the calibrated case. Multiple lines are individual channels. Individual channel responses are superimposed.

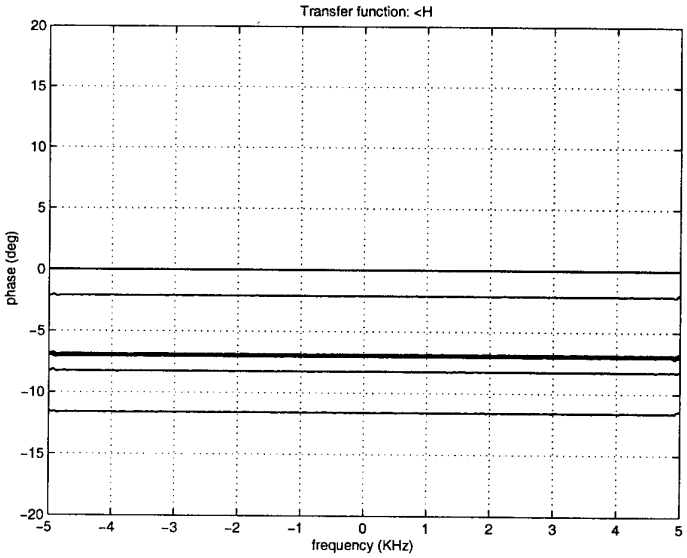

Figure 18: DDRX channel transfer functions (phase) (baseband freq. v. deg.) for the uncalibrated case. Multiple lines are individual channels.

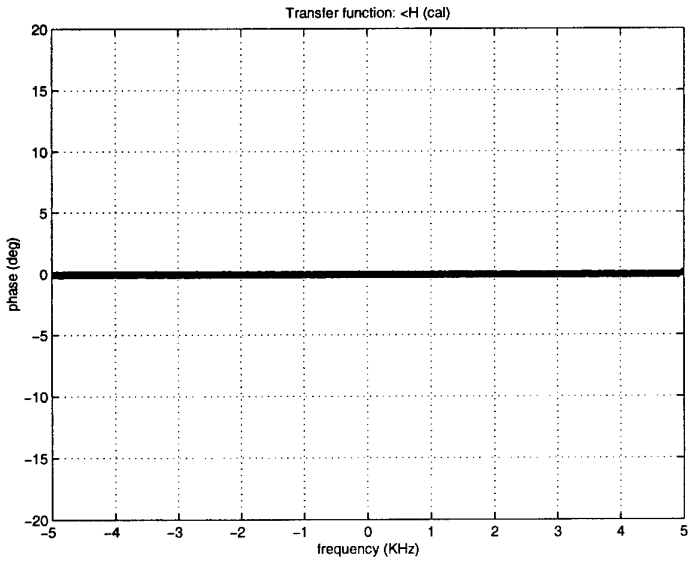

Figure 19: DDRX channel transfer functions (phase) (baseband freq. v. deg.) for the calibrated case. Multiple lines are individual channels. Individual channel responses are superimposed.

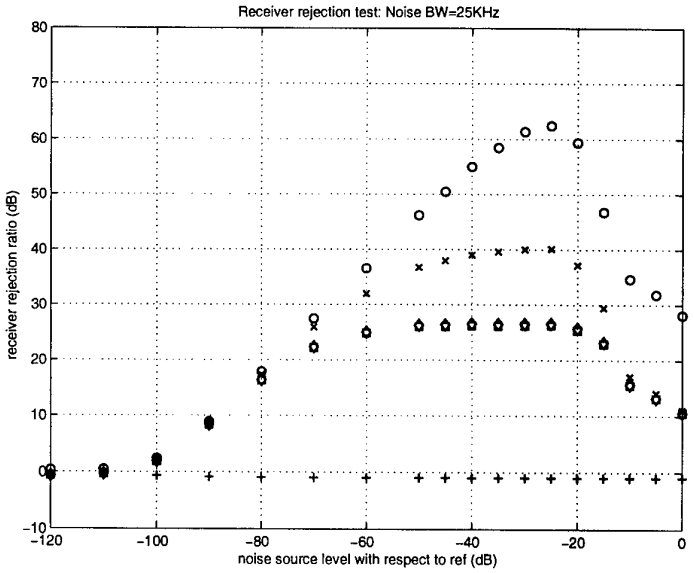

Figure 20: WJ9010 (`O`*) receiver rejection ratio. (+) uncalibrated plane wave rejection ratio. (*`box`*) calibrated (WJ-pre) plane wave rejection ratio. (*`diamond`*) calibrated (WJ-post) plane wave rejection ratio. (*`X`*) re-calibrated plane wave rejection ratio. Noise source bandwidth 25KHz.*

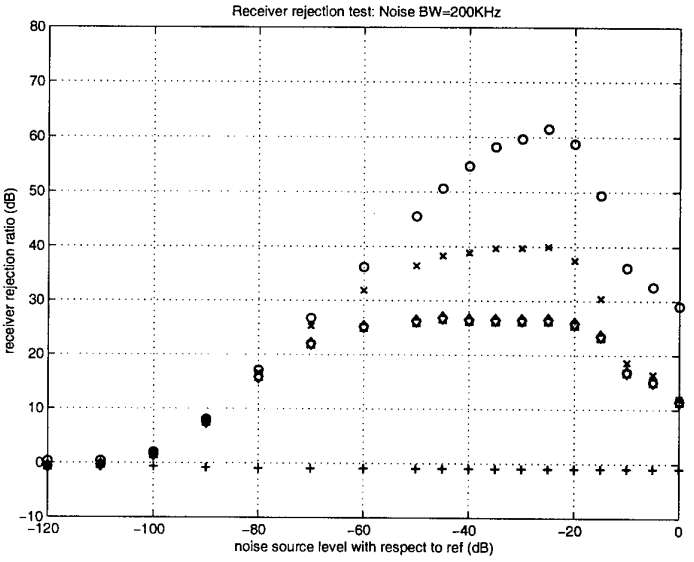

Figure 21: WJ9010 (`O`*) receiver rejection ratio. (+) uncalibrated plane wave rejection ratio. (*`box`*) calibrated (WJ-pre) plane wave rejection ratio. (*`diamond`*) calibrated (WJ-post) plane wave rejection ratio. (*`X`*) re-calibrated plane wave rejection ratio. Noise source bandwidth 200KHz.*

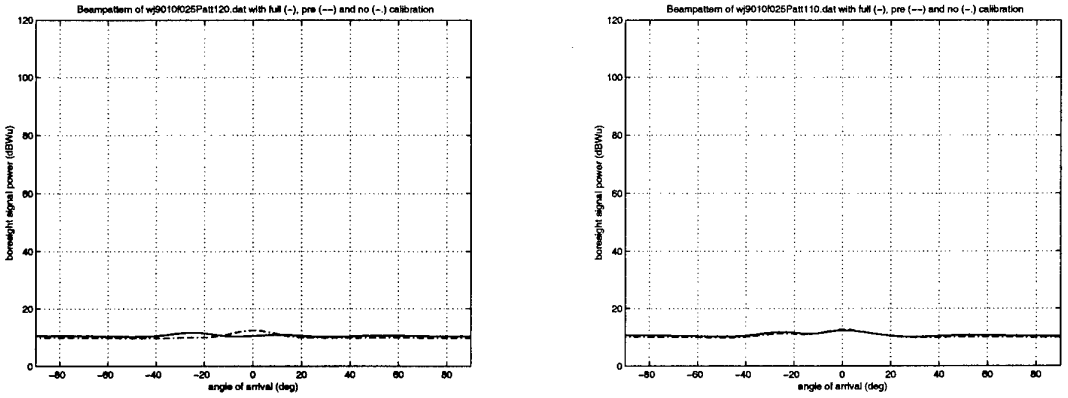

Figure 22: WJ9010 beampattern. Noise source input level (left) ref-120dB (right) ref-110dB. Noise source bandwidth 25KHz. (-.) uncalibrated. (--) calibrated (WJ-pre). (-) re-calibrated.

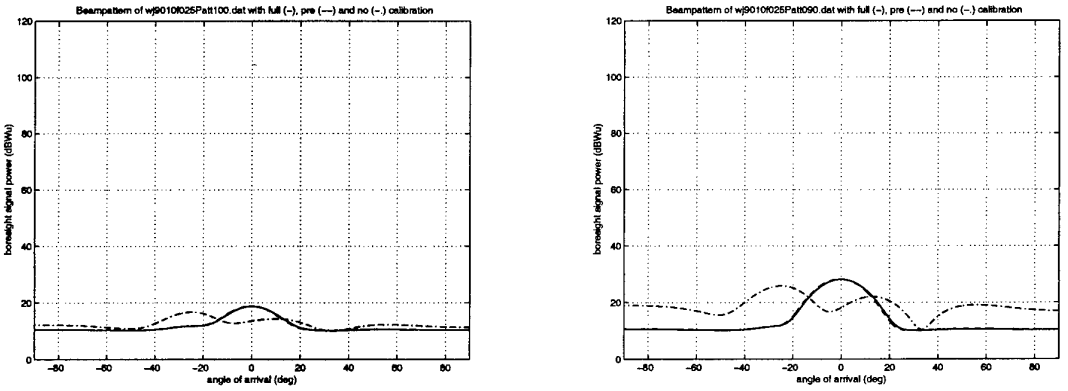

Figure 23: WJ9010 beampattern. Noise source input level (left) ref-100dB (right) ref-90dB. Noise source bandwidth 25KHz. (-.) uncalibrated. (--) calibrated (WJ-pre). (-) re-calibrated.

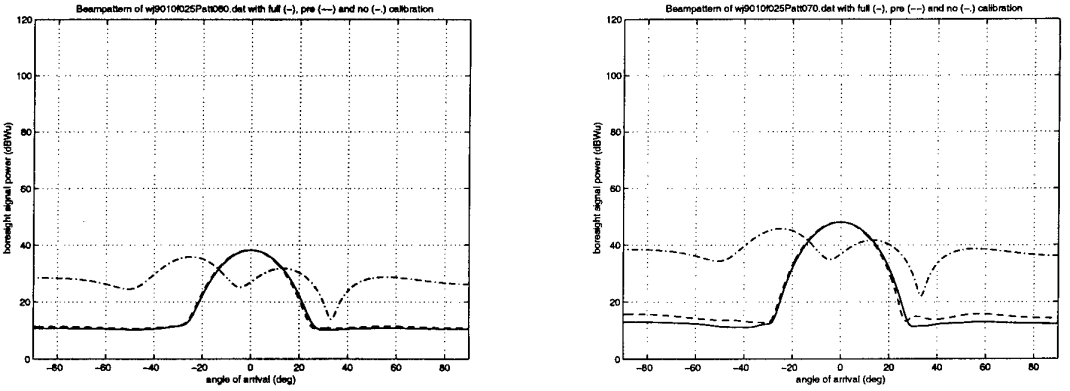

Figure 24: WJ9010 beampattern. Noise source input level (left) ref-80dB (right) ref-70dB. Noise source bandwidth 25KHz. (-.) uncalibrated. (--) calibrated (WJ-pre). (-) re-calibrated.

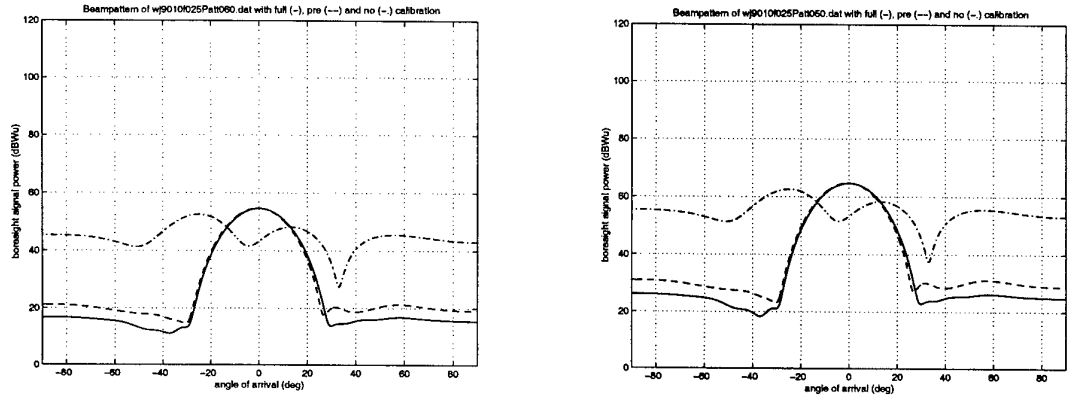

Figure 25: WJ9010 beampattern. Noise source input level (left) ref-60dB (right) ref-50dB. Noise source bandwidth 25KHz. (-.) uncalibrated. (--) calibrated (WJ-pre). (-) re-calibrated.

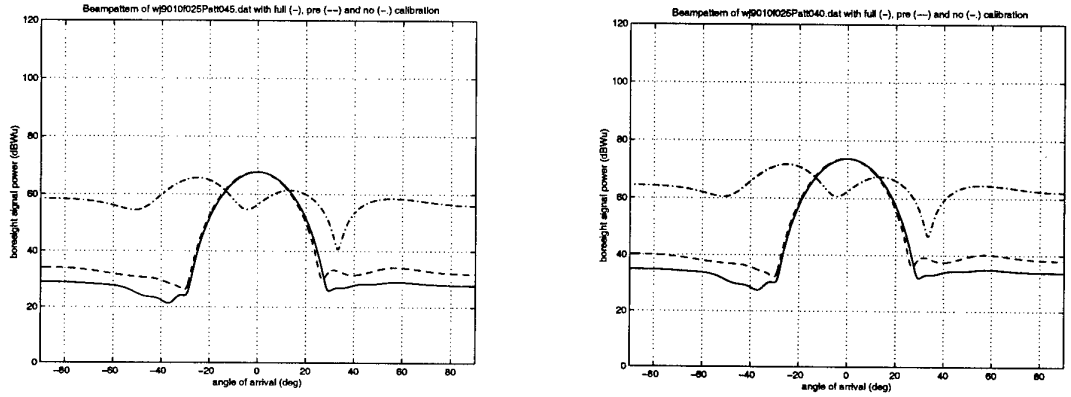

Figure 26: WJ9010 beampattern. Noise source input level (left) ref-45dB (right) ref-40dB. Noise source bandwidth 25KHz. (-.) uncalibrated. (--) calibrated (WJ-pre). (-) re-calibrated.

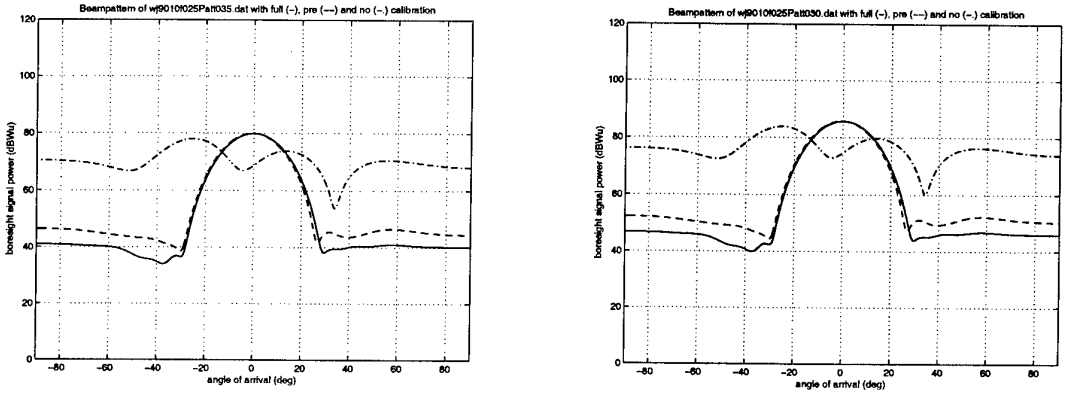

Figure 27: WJ9010 beampattern. Noise source input level (left) ref-35dB (right) ref-30dB. Noise source bandwidth 25KHz. (-.) uncalibrated. (--) calibrated (WJ-pre). (-) re-calibrated.

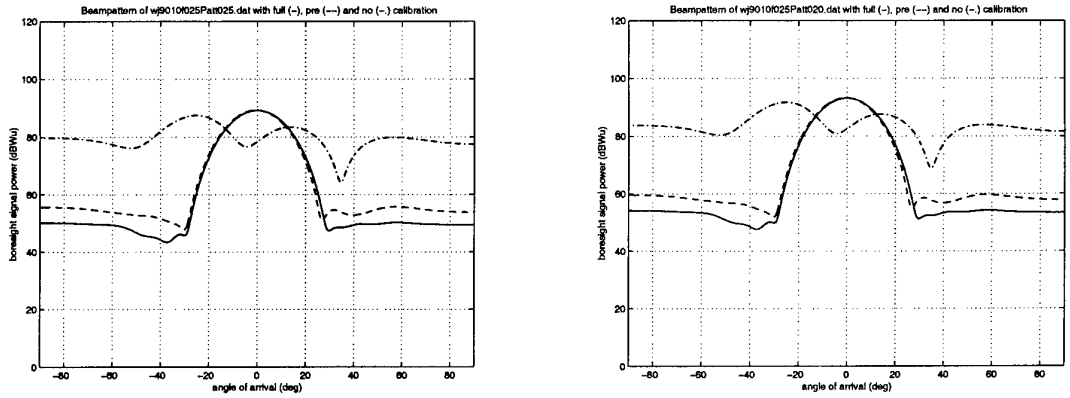

Figure 28: WJ9010 beampattern. Noise source input level (left) ref-25dB (right) ref-20dB. Noise source bandwidth 25KHz. (-.) uncalibrated. (--) calibrated (WJ-pre). (-) re-calibrated.

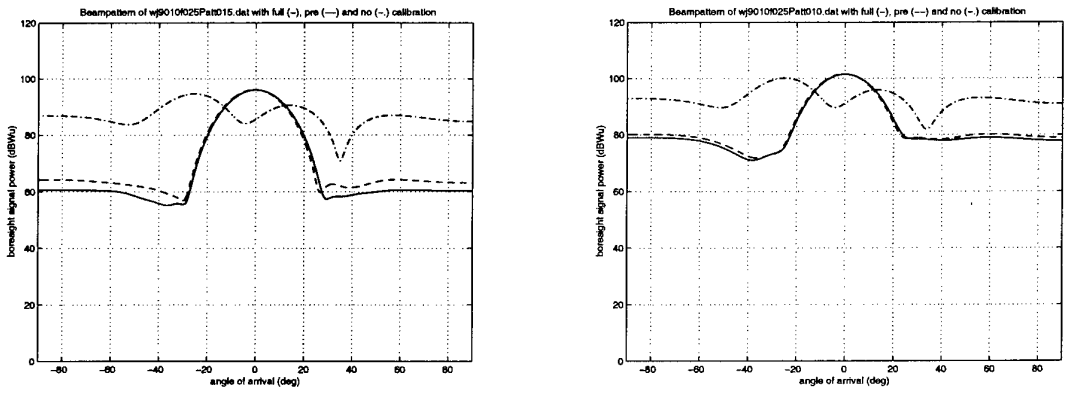

Figure 29: WJ9010 beampattern. Noise source input level (left) ref-15dB (right) ref-10dB. Noise source bandwidth 25KHz. (-.) uncalibrated. (--) calibrated (WJ-pre). (-) re-calibrated.

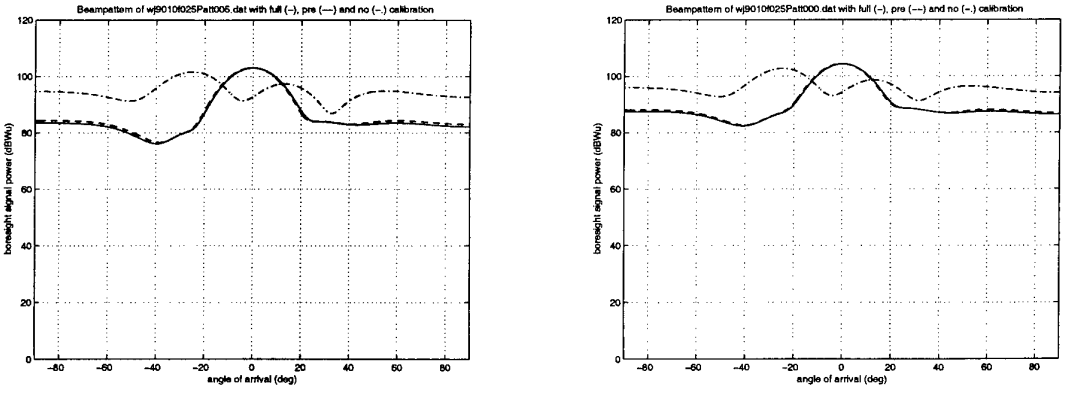

Figure 30: WJ9010 beampattern. Noise source input level (left) ref-5dB (right) ref-0dB. Noise source bandwidth 25KHz. (-.) uncalibrated. (--) calibrated (WJ-pre). (-) re-calibrated.

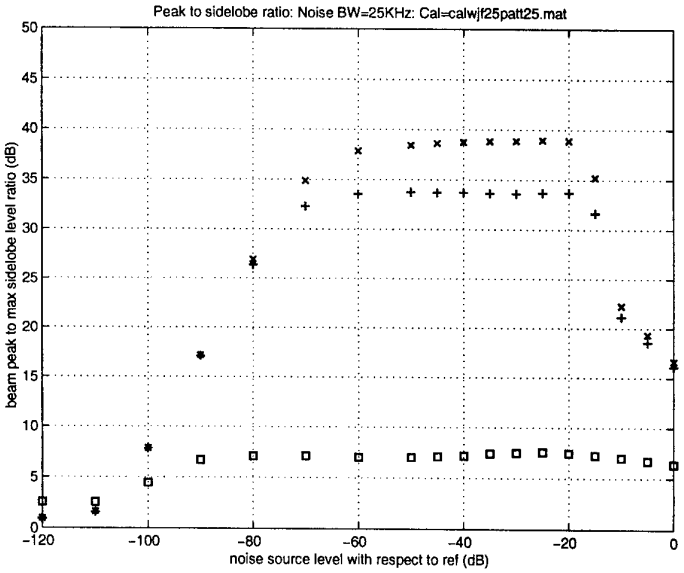

Figure 31: WJ9010 beam peak to maximum sidelobe level ratio for the (x) re-calibrated, (+) calibrated (WJ-pre) and (box) uncalibrated cases.

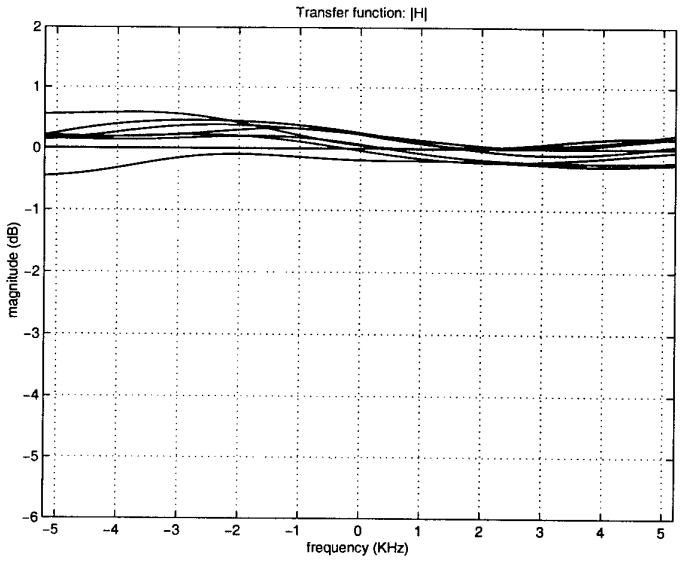

Figure 32: WJ9010 channel transfer functions (gain) (baseband freq. v. dB) for the pre-calibrated case. Multiple lines are individual channels.

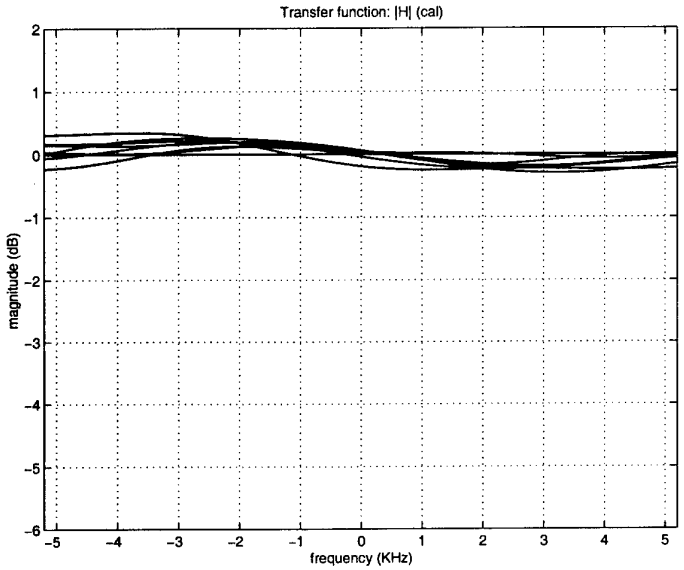

Figure 33: WJ9010 channel transfer functions (gain) (baseband freq. v. dB) for the re-calibrated case. Multiple lines are individual channels.

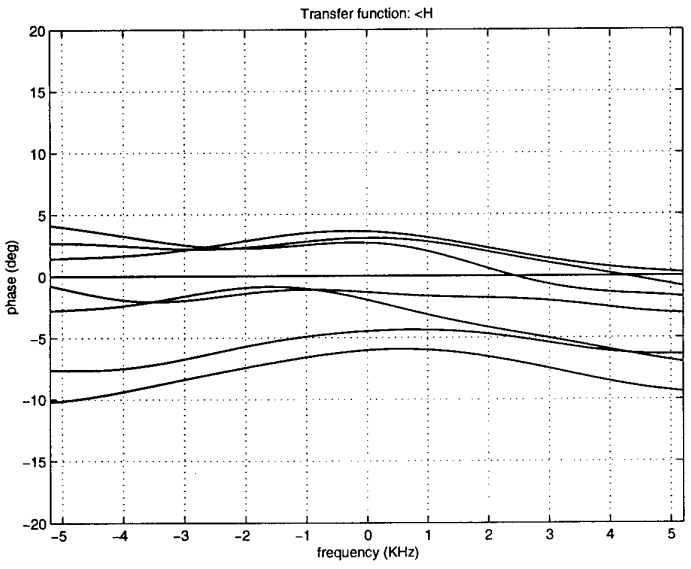

Figure 34: WJ9010 channel transfer functions (phase) (baseband freq. v. deg.) for the pre-calibrated case. Multiple lines are individual channels.

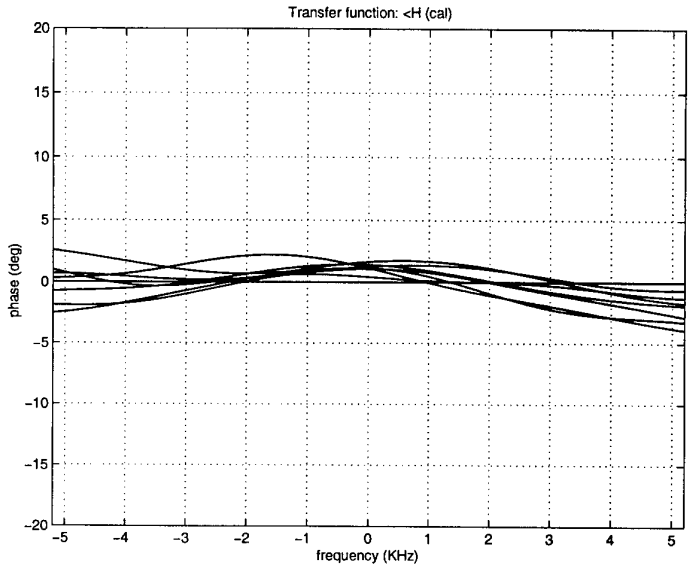

Figure 35: WJ9010 channel transfer functions (phase) (baseband freq. v. deg.) for the re-calibrated case. Multiple lines are individual channels.

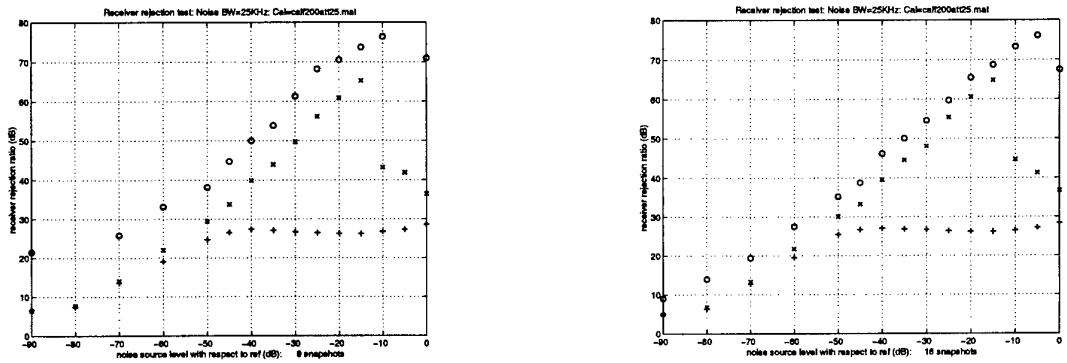

Figure 36: DDRX. (0) receiver rejection ratio. (+) uncalibrated plane wave rejection ratio. (X) calibrated plane wave rejection ratio. Noise source bandwidth 25KHz. The number of snapshots used to construct $\hat{\mathbf{R}}$ *is 9 (left) and 16 (right).*

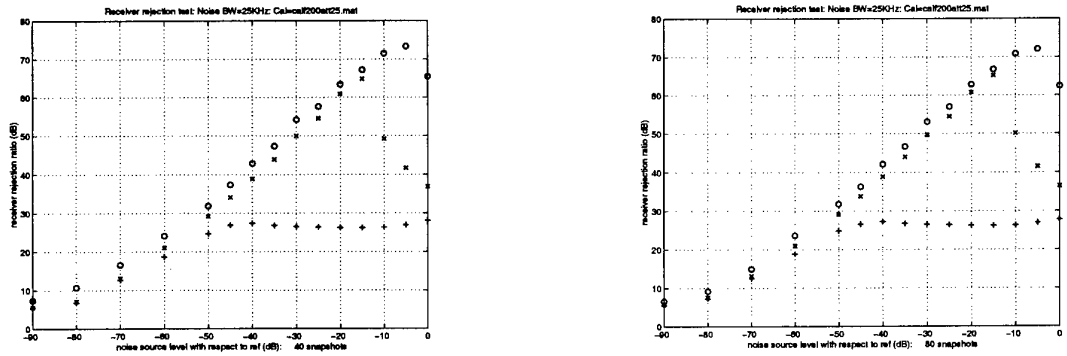

Figure 37: DDRX. (0) receiver rejection ratio. (+) uncalibrated plane wave rejection ratio. (X) calibrated plane wave rejection ratio. Noise source bandwidth 25KHz. The number of snapshots used to construct $\hat{\mathbf{R}}$ *is 40 (left) and 80 (right).*

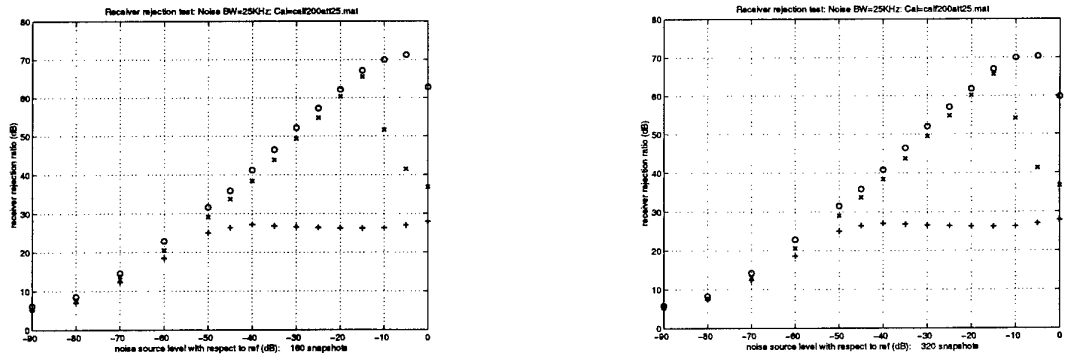

Figure 38: DDRX. (0) receiver rejection ratio. (+) uncalibrated plane wave rejection ratio. (X) calibrated plane wave rejection ratio. Noise source bandwidth 25KHz. The number of snapshots used to construct $\hat{\mathbf{R}}$ *is 160 (left) and 320 (right).*

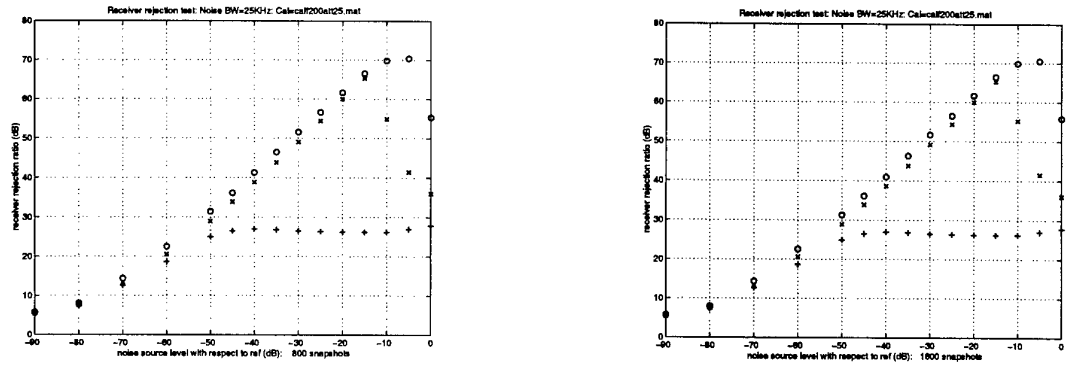

Figure 39: DDRX. (O) receiver rejection ratio. (+) uncalibrated plane wave rejection ratio. (X) calibrated plane wave rejection ratio. Noise source bandwidth 25KHz. The number of snapshots used to construct $\hat{\mathbf{R}}$ *is 800 (left) and 1600 (right). 800 is our recommended number of snapshots when testing the DDRX.*

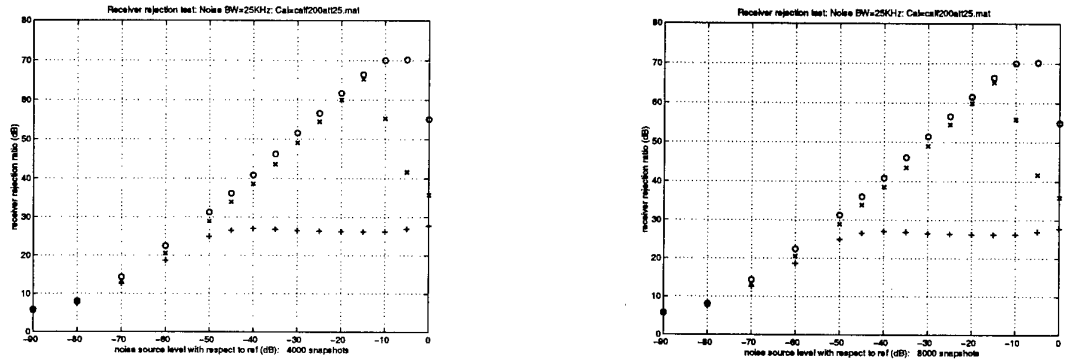

Figure 40: DDRX. (O) receiver rejection ratio. (+) uncalibrated plane wave rejection ratio. (X) calibrated plane wave rejection ratio. Noise source bandwidth 25KHz. The number of snapshots used to construct $\hat{\mathbf{R}}$ *is 4000 (left) and 8000 (right).*

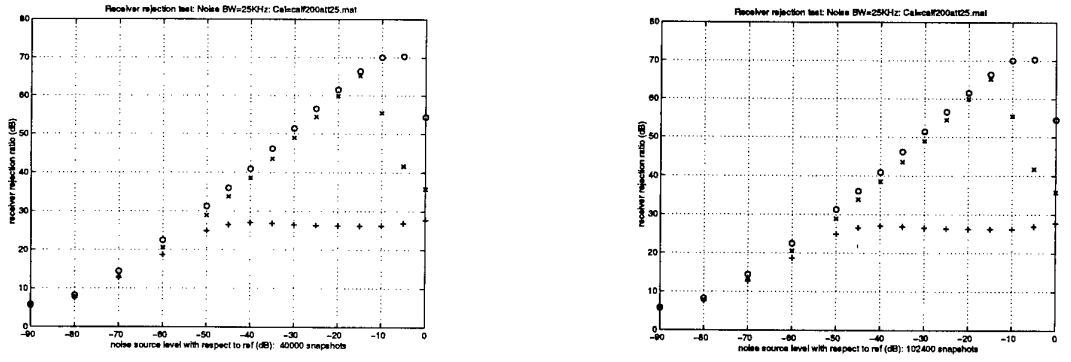

Figure 41: DDRX. (O) receiver rejection ratio. (+) uncalibrated plane wave rejection ratio. (X) calibrated plane wave rejection ratio. Noise source bandwidth 25KHz. The number of snapshots used to construct $\hat{\mathbf{R}}$ *is 40000 (left) and 102400 (right).*

DISTRIBUTION LIST

Quantifying Multi-channel Receiver Calibration

G. J. Frazer and Yu. I. Abramovich

	Number of Copies
DEFENCE ORGANISATION	
Task Sponsor	
Chief, Surveillance Systems Division	1
S&T Program	
Chief Defence Scientist FAS Science Policy AS Science Corporate Management	1
Director General Science Policy Development	1
Counsellor, Defence Science, London	Doc Data Sht
Counsellor, Defence Science, Washington	Doc Data Sht
Scientific Adviser to MRDC, Thailand	Doc Data Sht
Scientific Adviser Policy and Command	1
Navy Scientific Adviser	Doc Data Sht
Scientific Adviser, Army	Doc Data Sht
Air Force Scientific Adviser	1
Director Trials	1
Aeronautical and Maritime Research Laboratory	
Director, Aeronautical and Maritime Research Laboratory	1
Electronics and Surveillance Research Laboratory	
Director, Electronics and Surveillance Research Laboratory	Doc Data Sht
Surveillance Systems Division	
Research Leader, Wide Area Surveillance Branch	1
Head, Electromagnetics and Propagation Group	1
Head, Radio Frequency Projects Group	1
Head, Radar Signal Processing Group	1
Head, Surveillance Systems Integration Group	1
Dr G. J. Frazer	6
Prof. Y. Abramovich	1
Dr S. J. Anderson	1
Dr G. F. Earl	1
Dr M. Turley	1
Dr J. Praschifka	1

Mr G. Warne	1
Mr M. Tyler	1
Mr L. Durbridge	1
Mr M. Young	1
Mr R. Debnam	1
Communications Division	
Dr W. Marwood	1
Mr A. Massie	1
Mr D. Taylor	1
Mr I. Zahorvjko	1
DSTO Research Library and Archives	
Library Fishermans Bend	1
Library Maribyrnong	1
Library Salisbury	2
Australian Archives	1
Library, MOD, Pyrmont	Doc Data Sht
Library, MOD, HMAS Stirling	1
US Defense Technical Information Center	2
UK Defence Research Information Centre	2
Canada Defence Scientific Information Service	1
NZ Defence Information Centre	1
National Library of Australia	1
Capability Systems Staff	
Director General Maritime Development	Doc Data Sht
Director General Land Development	Doc Data Sht
Director General C3I Development	Doc Data Sht
Director General Aerospace Development	Doc Data Sht
Navy	
SO(Science), Director of Naval Warfare, Maritime Headquarters Annex, Garden Island	Doc Data Sht
Army	
ABCA Standardisation Officer, Puckapunyal	Doc Data Sht
SO(Science), DJFHQ(L), MILPO, Enoggera, Queensland 4057	Doc Data Sht
Air Force	
Officer Commanding 1RSU Detachment-A	1

Intelligence Program

DGSTA, Defence Intelligence Organisation	1
Manager, Information Centre, Defence Intelligence Organisation	1

Acquisitions Program

Corporate Support Program

Officer in Charge, TRS, Defence Regional Library, Canberra	1

UNIVERSITIES AND COLLEGES

Australian Defence Force Academy Library	1
Head of Aerospace and Mechanical Engineering, ADFA	1
Deakin University Library, Serials Section (M List)	1
Hargrave Library, Monash University	Doc Data Sht
Librarian, Flinders University	1

OTHER ORGANISATIONS

Telstra Applied Technology, Mr P. Kearsley	2
NASA (Canberra)	1
Info Australia	1
State Library of South Australia	1
Parliamentary Library of South Australia	1

ABSTRACTING AND INFORMATION ORGANISATIONS

Library, Chemical Abstracts Reference Service	1
Engineering Societies Library, US	1
Materials Information, Cambridge Scientific Abstracts, US	1
Documents Librarian, The Center for Research Libraries, US	1

INFORMATION EXCHANGE AGREEMENT PARTNERS

Acquisitions Unit, Science Reference and Information Service, UK	1
Library – Exchange Desk, National Institute of Standards and Technology, US	1
National Aerospace Laboratory, Japan	Doc Data Sht
National Aerospace Laboratory, Netherlands	Doc Data Sht

SPARES

DSTO Salisbury Research Library	5

Total number of copies: 70

DEFENCE SCIENCE AND TECHNOLOGY ORGANISATION DOCUMENT CONTROL DATA				1. CAVEAT/PRIVACY MARKING
2. TITLE Quantifying Multi-channel Receiver Calibration			3. SECURITY CLASSIFICATION Document (U) Title (U) Abstract (U)	
4. AUTHORS G. J. Frazer and Yu. I. Abramovich			5. CORPORATE AUTHOR Electronics and Surveillance Research Laboratory PO Box 1500 Salisbury, South Australia, Australia 5108	
6a. DSTO NUMBER DSTO–TR–1152	6b. AR NUMBER AR 011-867		6c. TYPE OF REPORT Technical Report	7. DOCUMENT DATE June, 2001
8. FILE NUMBER B9505-19-95	9. TASK NUMBER DST 95/034	10. SPONSOR CSSD	11. No OF PAGES 31	12. No OF REFS 8
13. URL OF ELECTRONIC VERSION http://www.dsto.defence.gov.au/corporate/reports/DSTO–TR–1152.pdf			14. RELEASE AUTHORITY Chief, Surveillance Systems Division	
15. SECONDARY RELEASE STATEMENT OF THIS DOCUMENT *Approved For Public Release* OVERSEAS ENQUIRIES OUTSIDE STATED LIMITATIONS SHOULD BE REFERRED THROUGH DOCUMENT EXCHANGE, PO BOX 1500, SALISBURY, SOUTH AUSTRALIA 5108				
16. DELIBERATE ANNOUNCEMENT No Limitations				
17. CITATION IN OTHER DOCUMENTS No Limitations				
18. DEFTEST DESCRIPTORS Multichannel Receiving Calibration Performance evaluation				
19. ABSTRACT A novel test has been developed for measuring the maximum achievable calibration performance of a multi-channel receiving system. The test may also be used to determine the quality of a particular calibration scheme and to rank the relative performance of several calibration schemes. The test provides a quantitive measure of the dynamic range of the multi-channel receiver. We demonstrate the utility of the test by analysing two different eight channel receiver systems.				

TECHNICAL REPORT DSTO-TR-1152 AR-011-867 JUNE 2001

ELECTRONICS AND SURVEILLANCE RESEARCH LABORATORY
PO BOX 1500 SALISBURY SOUTH AUSTRALIA, 5108
AUSTRALIA, TELEPHONE (08) 8259 5555